8-7-2004

Effect of Operating Parameters on the Growth Rate of Solution Grown Crystals

Kumar Vedantham

EFFECT OF OPERATING PARAMETERS ON THE GROWTH RATE OF SOLUTION GROWN CRYSTALS

By

Kumar Vedantham

A Thesis
Submitted to the Faculty of
Mississippi State University
in Partial Fulfillment of the Requirements
for the Degree of Master of Science
in Chemical Engineering
in the Dave C. Swalm School of Chemical Engineering

Mississippi State, Mississippi

August 2004

EFFECT OF OPERATING PARAMETERS ON THE GROWTH RATE OF

SOLUTION GROWN CRYSTALS

By

Kumar Vedantham

Approved:

_____	_____
Priscilla J. Hill Assistant Professor of Chemical Engineering (Director of Thesis and Major Professor)	Rudy E. Rogers Professor of Chemical Engineering (Committee Member)
_____	_____
Judy Schneider Assistant Professor of Mechanical Engineering (Committee Member)	Mark E. Zappi Texas Olefins Professor of Chemical Engineering (Graduate Coordinator of the Dave C. Swalm School of Chemical Engineering)

_____

Robert P. Taylor
Interim Dean of the College of Engineering

Name: Kumar Vedantham

Date of Degree: August 7, 2004

Institution: Mississippi State University

Major Field: Chemical Engineering

Major Professor and Director of Thesis: Dr. Priscilla Hill

Title of Study: EFFECT OF OPERATING PARAMETERS ON THE GROWTH RATE OF SOLUTION GROWN CRYSTALS

Pages in Study: 88

Candidate for Degree of Master of Science

In this work, crystallization experiments were carried out on four separate aqueous solutions of adipic acid, ammonium sulfate, urea and L-glutamic acid to measure the growth rate of these crystals under varying values of temperature, stirrer speed, cooling rate and holding time.

All experiments were carried out in the Mettler Toledo LabMax, which is an automated laboratory reactor. A polarized light microscope was used to capture the images of the crystals and Image Pro Plus software was used for the analysis of crystal samples.

Due to technical difficulties, the data could not be measured for adipic acid, ammonium sulfate or urea. L-Glutamic acid was much easier to work with and it was possible to obtain data. The growth rate for the β form of L-glutamic acid was estimated from the experimental data using a numerical simulation.

ACKNOWLEDGEMENTS

I would like to thank Dr. Priscilla J.Hill, my major professor for her valuable guidance and support through out my graduate program. I would also like to express my gratitude to Dr. Rudy Rogers and Dr. Judy Schneider of Mechanical Engineering department for being in my committee and providing valuable guidance and suggestion for my thesis. I would like to thank the Dave C. Swalm school of Chemical Engineering, Mississippi State University for sponsoring my research work.

TABLE OF CONTENTS

CHAPTER Page

LIST OF TABLES

LIST OF FIGURES

FIGURE Page

CHAPTER I

INTRODUCTION

Crystallization is the formation of solid particles within a homogeneous phase, where the solid molecules are arranged in a repeating lattice structure. It may occur as formation of solid particles in a vapor (as in snow), as solidification from a liquid melt (as in the manufacture of large single crystals), or as crystallization from liquid solution.

Crystallization is significant because it is widely used in many industries such as the pharmaceutical, fertilizer, dyes and pigments, biotech and other specialty chemicals industries. This technique must be performed in a controlled manner since it affects product quality. A product with uniform and narrow size distribution and large mean crystal size is often desired in industry. The industrial challenge is to produce crystals of the desired size and bulk density in the most economic manner.

Crystal morphology affects the efficiency of downstream processes (such as filtering, washing and drying) and influences material properties such as bulk density and mechanical strength, which play a major role in storage and handling. The morphology also affects the flowability, agglomeration and mixing characteristics of particulates (Doherty, 1998). Recently, polymorphs have gained importance in pharmaceutical industries. Polymorphs arise when molecules of a compound crystallize into chemically identical forms that are structurally different. This can

occur when molecules stack in the solid state in distinct ways, when molecules form different lattice structures, or when they have different lattice parameters.

Abbot Laboratories' produced a drug for patients with aids. But the drug developed a late-appearing polymorph that changed the shape from needles to big faceted crystals with different solubility properties (Rouhi, 2003). This difference in solubility of the drug can affect its bioavailability. Phenomenon like this makes crystallization an important issue in industry.

Though much work has been done on crystal size distribution and mechanisms to predict kinetics, relatively little work has been focused on crystal shape. One feature, which distinguishes crystals from most other particles, is their tendency to form well-defined shape. This is important for the measurement of their size since it places them between spherical particles and shapes that are usually complex. For most crystalline materials, the situation is further complicated since crystal shape changes with crystallization conditions such as temperature, supersaturation and purity.

In industry some form of habit modification procedure is necessary to control the type of crystal produced. This may be done by controlling the rate of crystallization; that is, by choosing the operating conditions such as the rate of cooling, the degree of supersaturation, the temperature, or the solvent; or by adjusting the solution pH, adding a habit modifier, or removing or deactivating some impurity that already exists in solution.

This work studies how the two compounds urea and L-glutamic acid form crystals under varying operating conditions. Urea is widely used in fertilizer

industries, and glutamic acid is an amino acid that exists in two chiral forms as L-glutamic acid and D-glutamic acid. For the present work the L form is taken. L-glutamic acid has two polymorphs - α and β. In this research, the desire is to produce the stable β form.

Table 1 gives an idea of the different crystal shapes obtained in industry and the problems associated with them. The optimum shape for industries would be a sphere as it can be easily filtered and transported. But in some cases other shapes are produced because the crystals might be more stable in that form. For example, the β form of L-glutamic acid is needle in shape, but still it is produced because that is the stable form in which glutamic acid can exist.

Chapter 2 provides a review of terminology used in crystallization and gives a brief literature survey of what has been done in this area. Chapter 3 focuses on the equipment and techniques involved in carrying out the experiments. Chapter 4 provides a detailed description of the experiments performed and discusses the data obtained from experiments. This is followed by the conclusion chapter.

Table 1: Different kinds of crystal shapes encountered in industries and problems associated with them

Crystal Shape	**Problems Encountered**
Long needle like type	Easily broken during centrifugation and drying
Flat, plate like	Low filtration rates
Cubical or other compact shapes	Caking
Complex or twinned crystals	Easily broken during transport

CHAPTER II

CRYSTALLIZATION THEORY AND BACKGROUND

2.1 Theory:

Before proceeding to the next chapter it is essential to know some of the crystallization terms that will be used often in this thesis. These include thermodynamic concepts such as solubility, supersaturation and metastable zone width, as well as kinetic concepts such as nucleation and growth.

2.1.1 Thermodynamics:

Solubility:

In order to operate a crystallizer, it is first necessary to know what conditions will produce crystallization. This information depends on solubility. Solubility is the maximum amount of solute that will dissolve in a given amount of solvent at a given temperature to produce a stable solution. When the maximum amount of solute has been dissolved in a solvent and the equilibrium is attained, then the solution is termed a saturated solution. The concentration of dissolved solute in a saturated solution is the same as the solubility of solute. If the solute concentration is less than the

saturation amount, the solution is subsaturated. If the solution contains more solute than the saturation amount then it is supersaturated.

Two factors that mainly control the solubility are pressure and temperature. Generally temperature is the major factor that influences the solubility of solids in liquids. This effect of temperature on solubility is governed by LeChatelier's principle, which states "a change in any of the factors determining an equilibrium will cause the system to adjust in order to reduce or counteract the effect of change" (Kotz and Purcell, 1991).

Before performing crystallization experiments, it is necessary to have the solubility data for the system of interest in order to prepare the saturated solution. The solvent plays a significant role in the system's solubility. For example, a compound's solubility in water may be very different from its solubility in alcohol. The solubility of urea in water at 20°C is 101 g per 100 g water, whereas the solubility in methyl alcohol is 22 g per 100 g methyl alcohol and in ethyl alcohol it is 5.4 g per 100 g ethyl alcohol at the same temperature.

Supersaturation:

A second factor in crystallization is the driving force or supersaturation. It is the concentration difference between that of supersaturated solution in which the crystal is growing and that of a saturated solution. "Supersaturation refers to the quantity of solute present in solution compared with the quantity which would be present if the solution were kept for a very long period of time with solid phase in contact with the solution" (Perry, 1997).

Generally, supersaturation is expressed in a number of ways (Mullin 2001) as shown below.

$$\Delta c = c - c^* \quad (1)$$

$$S = c / c^* \quad (2)$$

$$\sigma = \Delta c / c^* = S - 1 \quad (3)$$

where,

c is the solution concentration

c^* is the equilibrium saturation

S is the supersaturation ratio

Δc is the concentration driving force

σ is the absolute or relative supersaturation.

Each of these equations defines supersaturation in a different way. Eq. (1) express it as a concentration difference, while both Eqs. (2) and (3) express it as a ratio. One key difference is that in Eq. (1) it has the same units as concentration, while it is dimensionless in the other two cases.

Like supersaturation, concentration can also be expressed in many ways depending on whether or not the substance forms a hydrate and whether or not the solvent is water. Some expressions of concentration are as follows:

kg of anhydrous substance/kg of water

kg of anhydrous substance/kg of solution

kg of hydrate/kg of 'free' water

kg of anhydrous substance/m^3 of solution

kg of hydrate/m^3 of solution

kmol of anhydrous substance/m^3 of solution

When using concentrations, it is important to know which expression is used. For example, solubility data can be reported using any of these expressions.

Metastable Zone:

Nucleation cannot occur unless a solution is supersaturated. However, nucleation does not necessarily begin as soon a solution becomes supersaturated. The metastable zone refers to a supersaturated zone where nucleation is unlikely to occur. There is a limit as to how supersaturated the solution can be and still not nucleate. This is called the metastable limit. At concentrations above the metastable limit, nucleation is highly probable. Crystallizers are often operated in this region by the addition of a seed crystal.

The knowledge of the metastable zone width (MSZW) and the factors affecting it can be a major factor in the design of crystallization processes and may help to improve the reproducibility of the process. The temperature at which the first speck of particle appears corresponds to the width of the metastable zone.

The width of the metastable zone is calculated by the polythermal method. In this method a solution is cooled at a constant rate from a saturated temperature down to a temperature at which the first visible nuclei appears. The difference in these temperatures is generally termed as maximal supercooling (ΔT_{max}). Generally, the higher the zone width, the greater will be the stability of solution. To achieve a uniform crystal size distribution in batch crystallizers, they should be operated within

this metastable zone in a range where growth is supported and nucleation is negligible (Genck, 2000).

Much research has been done on the effect of impurities on crystal growth. Sayan and Ulrich (2001) studied the effect of Ca^{+2}, Mg^{+2}, Cr^{+3}, Fe^{+2} ions on the MSZW of boric acid. They concluded that the zone width decreased with the addition of impurities.

The MSZW for a particular compound varies with different operating conditions (Rajesh, et al., 2001). This was observed in all the experiments conducted for the present work with urea and glutamic acid where there was remarkable change in the temperature at which the first nuclei appeared when the cooling rate and stirrer speed was changed.

The seed crystal that is added influences the MSZW. Ramasamy, et al. (2001) studied the effect of addition of urea on the MSZW and nucleation parameters of ammonium dihydrogen orthophosphate. It was observed that at lower temperatures enhancement of zone width is good, but at higher temperatures the enhancement of zone width is narrow.

2.1.2 Crystallization Kinetics Mechanisms:

There are several mechanisms to account for changes in crystal size during crystallization: nucleation, growth, breakage, and agglomeration. Nucleation refers to the formation of a new crystal from solution, growth refers to the process of an existing crystal increasing in size, breakage refers to the fracture or attrition of a crystal, and agglomeration refers to two or more particles colliding and sticking

together. Since this work focuses on nucleation and growth, these mechanisms are discussed in more detail.

Nucleation:

Nucleation is the birth of a new particle, embryo or nucleus that act as a center of crystallization. Nucleation may occur spontaneously or it may be induced artificially by agitation, mechanical shock, friction, etc. Nucleation can be classified as shown in Figure 1.

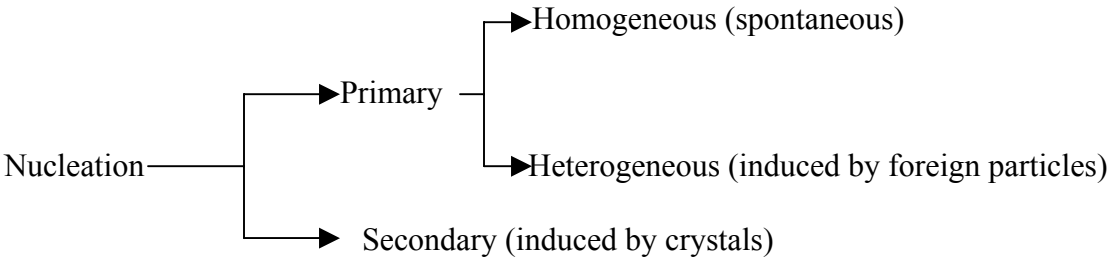

Figure 1: Types of nucleation

Homogeneous Nucleation:

Homogeneous nucleation is the formation of new particles without the influence of any solids including the wall of the container or even the minute particles of foreign substances. Supersaturation is the only driving force for nucleation of this sort to occur.

Nucleation occurs in several stages. Initially, several atoms or molecules in solution associate together to form a cluster. If enough particles associate together, then it marks the beginning of lattice arrangement and formation of separate phases called embryos. But sometimes these embryos are unstable and revert back to

clusters. However, if supersaturation is strong enough, an embryo can grow and become thermodynamically stable in solution. This stable form is called a nucleus, and this grows to form a crystal (McCabe et al., 1993). If a nucleus loses units it dissolves; if it gains units, it forms a crystal. This evolution of a crystal is explained by the following hierarchy.

Cluster → Embryos → Nuclei → Crystal

The fundamental expression for the rate of nucleation was first given by Volmer and Weber (Genck and Larson, 1972). They proposed an Arrhenius type relationship

$$B^0 = c \exp(-\Delta G^*/kT) \quad (4)$$

where,

ΔG^* is the free energy of formation of nucleus

k is the Boltzmann's constant

T is the absolute temperature

c is the proportionality constant

This expression incorporates the temperature effect into the nucleation rate. This expression is difficult to use because the free energy of formation of a nucleus is needed. The rate of nucleation can be also be expressed by

$$B^0 = A \exp[-(16\pi\gamma^3\nu^2) / (3k^3T^3(\ln S)^2)] \quad (5)$$

where,

B^0 is the rate of nucleation

S is the degree of supersaturation

γ is the interfacial tension

T is the absolute temperature

ν is the molecular volume

k is the Boltzmann constant

This expression incorporates the effects of both supersaturation and temperature.

Heterogeneous nucleation:

Heterogeneous nucleation is the formation of new crystal nuclei under the influence of foreign particles such as impurities. The size of these heteronuclei is important and it is found that the most active heteronuclei fall in the range of 0.1 to 1 μm (McCabe et al., 1993).

Secondary nucleation:

The formation of new crystals under the influence of existing macroscopic crystals in the mother liquor is called secondary nucleation or breeding of nuclei. There are different mechanisms by which secondary nucleation or breeding of nuclei can occur.

Initial breeding occurs when a crystal, which is not treated before, is introduced into a supersaturated solution. These are attributed to the impurity particles that are present on the surface of the seed crystal as the impurity particles are washed off and grow as new crystals. To avoid this an extensive pretreatment of the seed crystal is required.

Needle breeding occurs when a crystal is held stationary in a highly supersaturated solution, and needles or dendrites tend to grow out of the body of crystal, which in turn breaks off and cause breeding.

Polycrystalline breeding occurs at higher supersaturation where the crystal grows as a polycrystalline mass that breaks and gives rise to further crystals.

Collision breeding occurs when a crystal collides or slides into other solids in the supersaturated solution. This is the most common type of nucleation that occurs in most of the agitated seeded crystallizers. Supersaturation is the driving force, and the number of crystals increases with increase in supersaturation. Clontz and McCabe (1971) studied the growth mechanism of magnesium sulfate heptahydrate under collision breeding. It was inferred that instead of well formed normal crystals, abnormally grown dendrites formed as supersaturation increased. The aspect ratios of those crystals increased drastically at higher supersaturation. So it is observed that well-defined crystals were obtained only within a certain supersaturation range where collision breeding is active.

In addition to the various mechanisms, the factors affecting secondary nucleation must be considered. These may include:

- Degree of supersaturation:

  Since this is the driving force for crystallization, it is an important parameter in controlling the rate of nucleation. Increasing the supersaturation results in a larger nuclei population. Depending on the degree of nucleation, this can enhance crystallization or can produce too many fine particles.

- Temperature:

For many systems it has been found that nucleation decreases with increase in temperature. Therefore, this can be used to control the nucleation rate.

- Impurities:

  Impurities can either increase or decrease the solubility, which in turn affects the supersaturation. So a definite conclusion cannot be derived for the effect of impurities on nucleation. It depends on the system that is considered. For example, ammonium sulfate is very sensitive to impurities, and even a trace amount of impurity can alter its solubility data.

  Kitamura, et al. (1992) studied the effect of chromium ions on the crystal growth of ammonium sulfate. The growth rate of three faces (010), (100) and (001) faces were studied. It was seen that after a certain concentration of chromium was reached the growth ceased. This is achieved by the stepwise adsorption mechanism of chromium on the surface of crystal.

- Seeding:

  Seeding is the process of inducing crystallization by inoculating a supersaturated solution with small particles of the material to be crystallized. In industry, deliberate seeding is frequently employed to have control over the product size distribution. Generally, presence of seed increases the rate of nucleation and gives more reproducible results.

2.2 Crystal Shape:

The external appearance of a crystal, the crystal morphology, is partially dependent on the crystal habit. The crystal habit can be described in terms of faces,

their relative areas, the length of the axes in three directions, and the angles between the faces. The crystal morphology is often described by shape factors. The relative area is an essential factor that determines crystal habit. Two crystals that have the same face and internal structure can have different habit if the relative areas of the faces are not the same. Factors that influence the crystal habit and shape include the choice of solvent, the impurities and tailor made additives and the processing conditions under which crystals are grown. Crystal shape varies drastically with crystal growth rate and nucleation. Much research has been done to theoretically predict crystal morphology. Some of these methods are

1) Bravais-Friedel-Donnay-Harker (BFDH) method

2) Periodic bond chain theory

3) Attachment energy method

4) Issing temperature method

In all these theoretical methods only vapor-grown crystals were considered and the solvent effect was not considered (Mullin, 2001). But solvent can greatly influence the crystal habit by hindering the attachment of additional molecules.

2.3 Impurity Effect on Nucleation and Crystallization:

Any substance other than the one that is crystallizing is termed an impurity in crystallizing operations. According to this definition, even a solvent is termed an impurity and influences the whole process of crystallization. Impurities are generally present in the crystallizer or added on purpose (additives). It is important to understand the effect of these impurities in order to design tailor-made additives.

Impurities have a profound effect on growth rate of a crystal. The accepted mechanism for the effect of impurity or solvent on the growth rate is that they absorb on the face of a surface and decrease the growth rate. It is a well-known fact that slower growing faces always control shape. At slow growth rates, the shape of the crystal is determined by the thermodynamic equilibrium condition of a minimum value $\Sigma\sigma_i A_i$, where σ_i is the surface free energy and A_i is the corresponding area. Generally, this condition is rarely attained. So under real conditions the kinetics drives the final crystal shape more than thermodynamics (Winn, 1998).

There are three sites where an impurity can be absorbed on a crystal. It can be absorbed on a Kink, on a step or at a ledge or face of a crystal as shown in Figure 2. The effect is different for each of these different sites. Growth is affected even at a very low impurity level at a kink site. But more impurity is needed at a step site and face to see an effect on growth (Mullin, 2001).

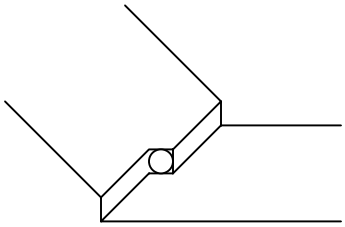

(a) Kink

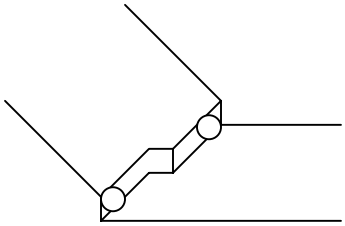

(b) Step

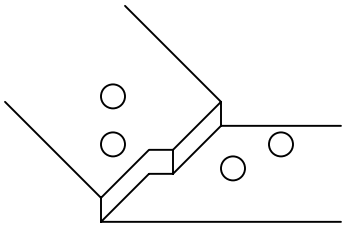

(c) Ledge or Face

Figure 2: Sites for impurity adsorption on a growing crystal (a) kink; (b) step; (c) ledge or face

2.3.1 Impurity Incorporation Mechanism:

Solvent or impurity effects also depend on the face of a crystal. Different faces exhibit different chemical properties because of the specific arrangement of molecules in the lattice. So each face exhibits specific chemical and structural attributes that affect the interaction with the solvents or impurity. For an impurity atom to attach to the crystal lattice, it has to physically displace the host molecules from their respective sites. This is not feasible unless the impurity is of the same size and chemical nature. If there are imperfections in the crystal lattice, then this condition is easily achieved. But in normal cases, it is hard for the impurity to achieve this type of bonding to the crystal lattice.

The other way is binding to the lattice without disturbing it. This occurs when the impurity interacts with the surface through van der Waals forces or through hydrogen bonding. Additives are generally selective in attaching to the faces. This type of bonding causes crystals to grow to a new shape, the case in low concentration impurities.

2.4 Types of Crystallizers:

There are different types of crystallizers used in industry. Crystallizers can be broadly classified as the following types:

- Batch or Discontinuous crystallizer:

A batch crystallizer is a closed vessel or a container where the feed is charged at the top and allowed to crystallize and the product taken out. The cooling can be done either by using atmospheric cooling without any stirring or by using artificial cooling with stirring. The equipment used for this work has artificial cooling, where a separate chiller is used to maintain and carry out the crystallization. The advantage of artificial cooling crystallizers over atmospheric cooling ones is that greater crystal density and corresponding smaller sizes are obtained. Also, aggregation is less and size distribution is more uniform. With batch crystallizers temperature control devices are essential since the large temperature drop across the cooling surface during early stages can cause scaling and reduces the cooling efficiency of the crystallizer (Mullin and Nylvt, 1971).

- Continuous crystallizer:

A continuous crystallizer is one where the feed is continuous fed into the unit and product is continuously removed. These crystallizers may be operated at steady state with a constant temperature and supersaturation. In general, seeding isn't required for continuous crystallizers except during start-up. The reason for this is that once they are running they always have crystals in them.

- Crystallization systems

In both batch and continuous crystallizers, the product from one crystallizer can be fed to the next, so that first crystallizer's product acts as seed for the second crystallizer. Both batch and continuous crystallizers can be operated in series and in parallel.

2.5 Crystal Growth:

Crystal growth consists of the following three basic steps:

- Diffusion of solute molecules from the bulk of the solution to the crystal-solution interface
- Reaction at surface where the solute molecules arrange themselves into crystal lattice
- Diffusion of heat of crystallization from the crystal solution interface back into the bulk of solution

In most crystallization processes the heat of crystallization is relatively low, and hence the effect of third step on the overall growth process is probably small compared to other two steps (Abegg, et al., 1968).

Crystal growth is generally governed by ΔL law of crystal growth proposed by McCabe. This law states that at uniform supersaturation and at the same temperature, all crystals are invariant and have the same growth rate independent of size (McCabe, 1993). This is called the ΔL law in crystallization, and it is a widely used generalization for crystal growth. It can be expressed as

$$\Delta L = G\Delta t \qquad (6)$$

The assumptions made in this law were that all crystals have the same shape, no nucleation occurs, no size classification occurs and the relative velocity between crystals and mother liquor remain constant. But in reality, growth rate is size-dependent and the relation that is most widely used expressing the size dependent growth rate is the Abegg, Stevens and Larson equation (Mullin, 2001).

$$G(L) = G_0 (1+\gamma L)^b \qquad b<1 \qquad (7)$$

where γ, b and G_0 are experimentally determined constants.

Larger crystals have higher growth rates if the process is diffusion controlled. This is because larger particles have higher terminal velocity. Crystals of near nucleic size have extremely slow rates because of lower supersaturation owing to their higher solubility. Another factor that determines the size dependent growth rate is the surface kinetics. Larger particle have more momentum because of their larger mass. Therefore they cause more surface damage when they collide.

2.6 Shape Factor:

Shape factors are dimensionless numbers that describe features of a particle's shape. They fall into two main classes. The simplest are those that may be calculated directly from geometric shape. For example, aspect ratios are ratios of characteristic lengths of particles. Frequently an equivalent sphere diameter is used. This equivalent sphere diameter is the diameter of a sphere that has a same volume as the particle of interest. Similarly, an equivalent sphere surface area is the surface area of a sphere with the same volume. Sphericity is defined as the ratio of the equivalent sphere surface area to a particle's surface area. Sphericity can be applied to finite particles of any shape.

The second class includes factors that emerge from the mathematical structure of a phenomenon or class of phenomena (Buffham, 2000). The behavior of imperfect crystals during size measurement cannot be analyzed using simple geometric arguments. The use of shape factor is one approach to quantify and relate the size of crystals with imperfection to near perfect crystals.

Morphology has an important effect on particle size measurement. For example, a sphere is the only object that is defined by a single size parameter, the diameter. For any deviation from sphericity, other size parameters must be accounted for, like the length, breadth and thickness. For this reason, a shape factor that is a combination of different size parameters is used (Pons, et al., 1999). These researchers studied the use of image analysis to quantify the morphology of particles. Basically, three steps that are needed to do this are visualization, image treatment and image characterization. In the visualization step the analog image as seen by human eye is transformed first into an electronic image by camera and then into a digital image. The next step in the image treatment removes any occlusions in the objects. The final step is the segmentation where the separation of the object of interest from the background is done. This is the critical step in the particle characterization. Some of the shape descriptors used are mentioned in the following Table 2.

Table 2: Some microscopical shape descriptors and their formula

SHAPE DESCRIPTOR	FORMULA	COMMENTS
Form factor	$P^2 / 4\pi S$ or $4\pi S / P^2$	This factor compares the surface of the object S to the surface of the disc of same perimeter (P)
Roundness	$4S / \pi F^2_{max} = D_{eq} / F_{max}$	Compares surface of the object S to the surface of the disc of same diameter F_{max}
Aspect Ratio	F_{max} / F_{min}	
Elongation	L_G / E	This is a substitute for aspect ratio for very elongated particle
Curl	F_{max} / L_G	For very elongated objects
Convexity	P / P_C	P_c is the perimeter of the convex bounding polygon
Solidity	S / S_c	S_c is the surface of the convex bounding polygon
Compactness	(Roundness)^0.5	

2.7 Background:

Crystallization is characterized by simultaneous occurrence of nucleation and crystal growth, which forms crystals of various sizes. Both the nucleation rate and the crystal growth rate are of primary importance in determining the crystal size distribution (CSD). Crystal growth and nucleation are important in design and sizing of crystallizers and therefore are important to finishing processes such as filtration, drying and centrifugation. Kulin, et al., (1997) used CSD analysis and growth rate to bypass the difficulties in determining nucleation kinetics for urea in water solution. Variation of shape with super-cooling of different temperatures was studied, and the shape was always needle-type for urea in water. The paper also discussed the effect

of stirring and suspension density on nucleation rate. Garside and Shah (1980) reviewed the crystallization kinetics research for many systems in continuous Mixed Suspension Mixed Product Removal (MSMPR) crystallizers. They discussed the effect of impurities, crystallizer hydrodynamics, temperature, supersaturation, and magma density on crystallizer kinetics.

Crystal Characterization:

A lot has been spoken about crystal characterization in recent past. Pons and Vivier (1991) used quantitative image analysis to obtain information on crystal shape either by individual analysis or by distribution. The paper discusses usage of image analysis and compares it with Fourier analysis and the geometric method.

C. J. Price (1993) observed the importance of particle characterization in order to determine crystallization kinetics. The various methods of characterizing crystals was mentioned with the advantages and disadvantages of every method. For batch crystallizers, a series of size distributions were measured and compared and from the differences between successive distribution, the growth rate and nucleation rate can be calculated. Also, Price (1993) worked on change of crystal habit and perfection with conditions such as temperature, supersaturation and purity and characterizing crystal shape. Optical microscopy permits measurements in the x, y, and z direction.

Sieving can also be used to characterize crystals if crystals are nearly perfect. However, nearly perfect crystals are rarely encountered and always effects of imperfections are considered. Information was given on different types of imperfections like adhering fragments, twinned, agglomerate and broken crystals. Image analysis gives the automated categorization on basis of number distributions.

It was mentioned that use of shape factors is one approach to quantify the effect of imperfections and trying to relate the imperfections to near perfect crystal. Recently, image analysis techniques have been applied to optical microscopy for morphological studies with the advantage that a large number of crystals can be surveyed (Maguin, 1993).

2.7.1 Crystal Habit Modeling

Winn and Doherty (1998) found a new technique for predicting the shape of solution-grown organic crystals. An approach was made to include the crystal shape in the overall design and organization of organic solids processes. The technique was successfully used to predict the shape of adipic acid grown from water, biphenyl from toluene and ibuprofen from polar and non-polar solvents. But the method they proposed was only applicable when there is dispersive or van der Waals forces between the solvent and crystal at kinks and steps or where there are known to be very specific electrostatic interactions (such as water-carboxyl group). This method cannot handle situations where forces are mostly coloumbic (such as inorganics) or where there is ionic bonding between solvent and crystal. The modeling also took into account of additives on crystal shape.

Urea:

Mougin, et al., (2002) used the *Ultrasonic Attenuation Spectroscopy* (UAS) technique to measure crystallization growth rates of urea from aqueous solution. It was seen that the particle size distribution (PSD) obtained by data inversion of UAS

gave some insight into shape of the formed crystal. It was observed that the bimodal distribution obtained from data inversion of UAS is due to the needle like shape of urea crystals.

Toyokura and Ohki (1991) investigated the growth of fixed needle crystals of urea and measured the latitudinal and longitudinal growth in a MSMPR crystallizer. Equations were proposed for estimating the CSD and mean longitudinal to latitudinal length ratio with a continuous MSMPR crystallizer, and thus concluded that the values obtained from the derived equation matched with the experimental ones.

Ammonium Sulfate:

Bamforth (1974) studied the effect of attrition and breakage on crystal shape of ammonium sulfate. Also, Bamforth deals with the effect of impurities on crystal shape. Kubota, et al., (2000) studied the combined influence of supersaturation and impurity concentration on crystal growth. The growth behavior of ammonium sulfate was analyzed numerically. Kitamura, et al., (1992) observed that impurities have a tremendous influence on habit of crystals. The shape of ammonium sulfate crystals is modified even by small traces of impurity. It was observed that crystal growth rate was greatly reduced by the presence of chromium ions.

Glutamic Acid:

Mougin, et al., (2002) used the *Ultrasonic Attenuation Spectroscopy* (UAS) to determine particle size during the crystallization of L-glutamic acid in its two polymorphic forms. Both α and β forms are orthorhombic where the length of each

face is different and the angle between the edges of each face is 90°. It is mentioned that the α form can be achieved by rapid cooling of aqueous solution of L-glutamic acid. Under fast cooling rates (0.75°C/min and 0.4°C/min) and cooling up to 15°C the α form is found to be predominant, but at 0.1°C/min the β form is favored. The crystallization of both forms is discussed separately. For the α form at 25.4°C and 0.75°C/min, the mean size was 2.6 μm, but at 21.1°C a bimodal distribution due to secondary nucleation was obtained with a mean size of 180 μm. For β particles, the distribution is bimodal throughout. Unlike the α particles whose bimodal distribution reflects a tail of finer particles commonly found at the end of crystallization, the modes of distribution of β particles do not evolve independently of each other. This can be seen from the ratio of geometric mean throughout the crystallization. At the beginning, this ratio is higher but otherwise it is constant throughout the process. The length of the crystals is around 200 μm and width is around 15-40 μm.

Kitamura and Ishizu (1999) studied the growth kinetics and morphological change of α and β crystals of L-glutamic acid using the single crystal method. The growth rate of both α and β crystals is by the *Nuclei above Nuclei* (NAN) mechanism. Crystallization of polymorphs depends on temperature. With a decrease in temperature, α crystals are formed. It is observed that solution velocity does not affect the growth rate, and the growth is controlled by the surface reaction process. The morphological change of the α crystal during growth is observed, i.e. the shape of crystal changed from rhomboid to hexagonal and thickness of crystal increases with supersaturation. The growth of β is mostly in the x (1 0 0) direction, and it is

less in the y (0 1 0) and z (0 0 1) directions. It is concluded that morphological change of α crystals is due to differences in dependence of growth rate on super-saturation between (1 1 1) and (1 1 0) faces. The higher growth rate of α was due to a large kinetic factor and a low edge free energy of α.

Kitamura (2002) also investigated the effect of L-Phenylalanine on the growth rates and morphologies of L-glutamic acid and L-histidine by the single crystal method. It is noticed that the temperature effect on shape was seen only in some polymorphs. For example, temperature does not influence polymorphs of L-hystidine, and this is due to the difference in molecular orientation between the polymorphs.

Kitamura and Ishizu (1998) studied the additive effect of L-Phenylalanine(L-Phe) on growth kinetics of L-glutamic acid. It is inferred that at 318 K with L-phenylalanine the precipitation of β crystal is suppressed, suggesting L-Phe preferentially suppresses both nucleation and growth rate of β L-glutamic acid. But at 298 K, crystallization rates of α crystals are retarded and morphological change of α crystals are induced. With increase in L-Phenylalanine concentration, more than 3.9E-04 mol/l growth rate becomes irregular. This suggests that the growing process of L-glutamic acid becomes complicated because the adsorption of L-Phenylalanine is not uniform all over the crystal surface. At constant L-Phenylalanine concentration the growth increases with increase in supersaturation. For α crystals, growth rate was affected only in the x (1 0 0) direction.

Regarding glutamic acid, most of the reported work focused on the transformation from unstable alpha form to the stable beta form. Though it is a well-

known fact that alpha form is preferred in industries due to its ease of separation from mother liquor (Mougin 2002), it is essential to know the growth characteristics of beta form since lower cooling rates produce beta form. There are data published for the growth rate of alpha form but no such data exist for beta form. Only the facial growth on a single crystal was studied before and no work has been done on a bulk of crystals as explained before in this chapter.

CHAPTER III

EXPERIMENTAL METHODS AND MATERIALS

This research includes the formation of crystals from supersaturated solutions and the analysis of the resulting crystals. The equipment and the experimental techniques used are described in detail in this chapter.

This discussion is divided in-to two major sections

- Crystallization and sampling
- Analysis

The crystallization and sampling section discusses the particle formation procedures, while the analysis section discusses the analysis of the particles

3.1 Crystallization and Sampling

3.1.1 Major Equipment:

LabMax:

The Mettler Toledo LabMax is a laboratory reactor that is used to perform chemical reactions automatically. It is designed in accordance with state-of-the-art technology with regard to safety and product quality. This automated reactor is controlled and run by CAMILE TG software. It includes a reactor with a stirrer, a

computer and sensors for data acquisition, and temperature control.

Reactor:

The reactor is made up of a 1 liter jacketed glass vessel and can operate at ambient pressure and at a vacuum of 50 mbar. It includes a PT-100 temperature sensor and a glass stirrer. It has ports in the top for analysis equipment and a valve at the bottom to remove the vessel contents. A collection tray is installed below the reactor and serves to collect reactor contents. There is a plastic shield in front of the reactor vessel to protect the reactor from damage and to prevent the user from contact with the hot reactor. Figure 4 shows the LabMax unit with the stirrer motor mounted above the reactor vessel. The stirrer can be set to run at speeds up to 850 rpm.

The computer includes a flexible menu driven program for operating LabMax. Specifically, it allows the user to determine what operations the unit will perform during an experiment. It can be programmed as a series of steps where variables such as the temperature, agitation rate, and operating time of each step can be set. It also allows the user to set safety parameters. For example, if the temperature goes above or below set limits, the experiment will automatically abort. The computer also collects data during operation. Figure 3 shows the schematic diagram of the entire process.

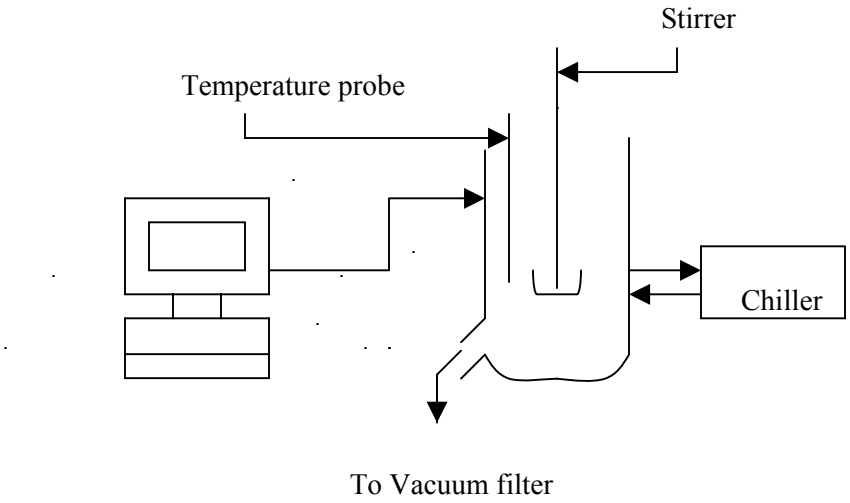

Figure 3: Schematic diagram of the process

For proper operation, process control is important. In fact, it is critical to control the temperature of the vessel contents since solution crystallization can be sensitive to temperature. The LabMax control system basically comprises the 3 modules:

- Thermostatting unit
- Controller unit
- Thermostat

Each one of these is described below in more detail.

The thermostatting unit is located between the sensors and the computer. It includes a microprocessor control, the measurement system and the power electronics and electromechanical control. The microprocessor receives parameters and set values from the computer, acquires measured values from the sensors, and controls the temperature and stirrer speed in the reactor. If the connection to the PC is

interrupted the microprocessor adjusts the temperature to the predefined default value.

The controller unit is used to control the pumps, valves and other external devices; and to acquire additional measurement data. This unit includes a microprocessor system that measures inputs and outputs for measured value sensors. The microprocessors of the external devices receive a set of measured values (temperature of reactor contents, oil temperature, coolant temperature, stirrer speed) every two seconds. The controller unit controls the dosing operations and pH. The dosing operations were not used for this work.

The thermostat controls the temperature of the reactor contents. Silicon oil, which is used as heat transfer medium, is pumped through the jacket of the reactor to keep the temperature at the set value.

Chiller:

Since LabMax does not have a built in cooling unit, cooling fluid must be supplied. A Julabo chiller was used to provide cooling fluid for the LabMax. The chiller has provisions to enter the high temperature limit (up to a limit of 400°C), low temperature limit (down to a limit of -50°C) and working temperatures.

3.1.2 Labmax Operation:

Safety parameter values need to be set before programming the experiment. Safety parameter values define the operating limits of the LabMax unit. If the

experimental conditions go beyond the safety parameters, then the program will abort the experiment.

Next the experiment is programmed into LabMax. It is programmed as a series of steps or stages. Any number of stages can be set for an experiment and the LabMax performs each stage consecutively in the order in which it is entered. For each stage of the experiment, the reactor temperature, stirrer speed and duration of the stage is set and varied accordingly to requirement of the experiment. There are options to view and modify the program and save it when it is modified. If the data entered in the program is out of the range of safety parameters, then an emergency program is triggered.

Figure 4: The Mettler Toledo LabMax (automated laboratory reactor) with the Chiller to its side

3.2 Preparation of Saturated Solution:

To prepare a saturated solution at a given temperature, the solubility at the given temperature is used. A fixed amount of solvent is added to the vessel; and then the amount of solute required to saturate the solution is added. The solution is heated above the saturation temperature and held at this elevated temperature to ensure that all of the solute dissolves. Then the solution is gradually cooled to the saturation temperature.

For illustration purposes, consider the case where a saturated solution of urea in water is prepared for a saturation temperature of 30.7°C. The solubility of urea at this temperature is 162 g/100 g water (Seidell, 1928). About 203.1g of urea and 150g of deionized water are weighed using an electronic balance that has accuracy up to two decimal places and added to the reactor vessel. Deionized water is used for the experiment since the presence of impurities in the water may affect the shape of crystals formed and the solubility. The vessel contents are then heated above 30.7°C to dissolve all of the solids. Then the vessel is gradually cooled to 30.7°C to form a saturated solution.

In all the runs that were performed the reactor contents were taken 10-15 °C ahead of the saturation temperature to make sure the contents are completely dissolved. This value is completely dependent on the system studied. Since urea is readily soluble in water an increase of 10-15°C is enough but for substance like ammonium sulphate we may have to take to 30 – 35°C more than saturation temperature. After the contents are dissolved the reactor is cooled at a desired rate

and stirrer speed set in the recipe. About 0.04 gms of urea was seeded in the reactor for all the experiments at 29°C. A filter flask connected to the vacuum filter was placed below the stopcock at the bottom of the reactor vessel. Once the desired temperature was reached the stopcock was opened and turning on the vacuum filter filtered a small sample of the contents. The sample was taken for at least at two different temperatures for a given set of operating conditions in order to make comparisons. The collected sample is then taken for microanalysis.

3.3 General Procedure for Crystallization Experiment:

Step 1:

A mixture of solute and solvent is prepared that is saturated at the set saturation temperature. The amount of solute needed for 150 g of deionized water is calculated and weighed and then added to the vessel. A funnel is used for adding the solute to the reactor vessel. Then the deionized water is weighed and added to vessel.

Step 2:

The next step is to program the LabMax. The stirrer speed was set as desired. The mixture was heated to 10°C – 15°C above the saturation temperature and given around 40 minutes to heat. Then the contents are held at this temperature for around 20 min just to make sure that the solute is completely dissolved. Some substances do not dissolve immediately and need to be maintained above saturation temperature for some time before everything can be dissolved. The solution is then gradually cooled to the saturation temperature. If seeding is used, the seeds are added at the saturation

temperature. The solution was then cooled to the desired final temperature at the desired cooling rate. The reactor vessels are observed to see if anything crystallizes before the saturation temperature. If there is some problem with the way the experiment is conducted; the experiment is then repeated from step 1. At the saturation temperature, a small sample of liquid (about 2 ml) is taken with the help of syringe from reactor and added to the sample bottle. The sample bottle is prepared as described in the following section 3.4.

Step 3:

At the end of operation, the slurry is held at the temperature at which the sample is to be taken. The stopcock at the bottom of the vessel is opened and material is taken and filtered. The stopcock is left opened until enough material is collected. The filtration apparatus is already set up just beneath the nozzle from which the sample is taken and the contents pass directly to the filter from the LabMax as shown in Figure 6.

Step 4:

Finally the solid sample was prepared for microanalysis as mentioned later in this chapter in slide preparation section. The above-mentioned procedure can be used for any material by changing the saturation temperature and other operating parameters as desired for the experiment.

3.4 Concentration Measurements

A density meter (Anton Parr DMA 4500) as shown in Figure 5 was used to find the concentration of the solution at the saturation temperature. Density data for ammonium sulfate was taken from CRC handbook of chemistry. Our experimental procedure was verified by checking the density of the solution to see whether it coincided with the data from literature. This procedure consisted of three steps: preparation of the sample bottle, taking the sample, and analyzing the sample in the density meter.

Sample bottle preparation:

Normally, a sample would be added to an empty sample bottle. However, since samples from the crystallizer are often above room temperature, there was a possibility of crystal formation in the sample bottle as the sample cooled. To prevent this, the sample was diluted. Also the density readings were taken at 20°C inside the density meter, which is again much less than the reactor temperature and could support crystal formation. So required amount of water was weighed and added to avoid this crystal formation.

The sample was diluted by the following procedure. An empty sample bottle was weighed. Then the amount of water needed to avoid crystallization was calculated. The required amount of water was added along with additional half milliliter of water. Then the bottle is weighed with the water. This was done to determine the amount of dilution.

Sampling procedure:

The sample is taken from the reactor with a syringe. Immediately it is injected in to the sample bottle with water. Now the bottle is weighed with the sample. The mixture is allowed to cool and then injected in to the density meter for readings. Three such bottles were prepared. It is a common practice to rinse the density meter with deionized water after getting each reading in order to get an accurate result.

Figure 5: Anton Parr density meter with a syringe in the side that feeds the sample in to it.

3.5 Filtration Unit:

In order to avoid any crystals coming out or growing on the filter paper, filtration must be done quickly. Vacuum filtration was preferred to other types of filtration since it had to be accomplished quickly. A standard filtering funnel was placed on a filtering flask. The filtering flask was connected to the vacuum filter and was placed below the stopcock at the bottom of the reactor vessel. Once the desired temperature was reached, the vessel stopcock was opened to transfer the vessel contents to the filtering funnel. The opening of stopcock and turning on the vacuum pump must be done simultaneously to make the filtration process quick. A 90mm diameter filter paper was used with a pore size that could retain particles larger than 7 microns.

Figure 6: Filtration assembly

3.6 Analysis

Our aim is to measure the size and shape of crystals. So to measure the shape a Polarized Light Microscope was used. The following paragraphs describe each one in detail.

3.6.1 Polarizing Light Microscope (PLM):

A polarized light microscope is used for the enhancement of images. An Olympus BX51 polarizing light microscope was used to capture crystal images. The microscope has a DP12 camera at the top, which records the magnified images and sends it to a digital camera adapter that can be used with the microscope. The adapter stores all the images in a smart media card, which is a storage device. The DP12 has a LCD monitor through which the magnified image of the crystal that is being focused can be viewed simultaneously. It gives a clear idea of how the picture might look after it is sent to the computer and downloaded for analysis. The mode button allows the user to record pictures and play them back later. The pictures can be downloaded to a computer that is connected to the DP12 control box or getting real time images. The DP12 control box allows the user to erase images after downloading to provide memory space for storing images for further use. There is a digital display of number of pictures recorded in the media card. An image can also be protected from erasing through AE lock protect button in the control box. After focusing the image to required accuracy, the expose button at the bottom of the control box is pressed to record the image on the media card. These images are then

transferred to a computer for image analysis. Figure 7 shows the picture of a Polarized Light Microscope that was used for the present work.

Figure 7: Polarized Light Microscope (PLM) with a DP12 camera at the top

3.6.2 Image Pro Plus:

Image Pro Plus gives the state of art imaging and analysis capability for acquiring, enhancing and analyzing your images. Some of the features include:

- Acquisition of image data from a camera, microscope, or scanner

- Image enhancement using powerful color and contrast filters, morphology, field flattening, background subtraction and other spatial and geometric operations.
- Tracing and counting of objects manually and automatically. Measurement of object attributes such as area, perimeter, aspect ratio and roundness. Calibration of spatial scale to any unit of measure.
- Viewing collected data numerically, statistically or in graphic form and saving it to a disk.
- Extraction features with spatial tools that isolate an Area of Interest (AOI) from the rest of the image, or with segmentation tools that extract features by color or intensity value.

In this work only acquisition, calibration, extraction, measurement, and counting operations of Image Pro Plus were used. The calibration was done by viewing a stage micrometer. This is a slide that is marked in microns. The stage micrometer used had a marking 1 mm long with divisions of 0.01 mm. The calibration is saved as a file. The final results were exported to MS Excel.

3.6.3 Slide Preparation:

Keeping the sample at room temperature for 5-6 hrs dries the sample from the crystallizer. The dried crystal sample is then transferred to a microscopic slide to get a clear image of the crystal. Images cannot be taken directly from the filter paper as crystals might be lying one above the other and a clear image cannot be obtained.

Care should be taken not to break the crystals while transferring from filter paper to slide. The slide is completely dry when the sample is put on it.

3.6.4 Measurements Procedure:

The slide is observed under a Polarized Light Microscope. The magnification used for urea, ammonium sulfate, and glutamic acid crystals was 100x. Since urea crystals were much bigger it was not possible to take pictures at higher magnifications. The crystal images were captured using a DP12 digital camera on top of the microscope. The images were then transferred to the computer that has Image Pro software.

Since the image analysis requires calibration, an image of the stage micrometer at 100x was used to calibrate the software. Then the crystal image was opened and from the measure menu in the software the calibration was checked to see whether it matched the magnification with which the pictures were taken. The measure menu was chosen and the parameters to be measured like area, aspect ratio, major axis, minor axis were selected. Then the crystals were colored by using select color option and then the counting was done. Coloring was done in order to separate the actual sample from the background. Options were available in the edit menu to split two objects and merge objects. The data was directly transferred to an excel file and was saved for future reference. The transferred data was then grouped according to various size ranges in order to find the number fraction. A graph was plotted between the number fraction and size range for data collected at various temperatures in order to see the growth occurring at various temperatures.

CHAPTER IV

RESULTS AND DISCUSSION

Experiments were conducted for several systems. In each case there was one solute with water as the solvent. While the adipic acid/water, ammonium sulfate/water, and urea/water systems did not work well experimentally, the L-glutamic acid/water system gave meaningful results. Each system is discussed in more detail individually.

4.1 Adipic acid

In a crystallizer the four mechanisms of growth, nucleation, agglomeration, and breakage can occur. In this thesis, the goal is to study growth and nucleation. It is much easier to do this if agglomeration and breakage are negligible for a system.

Adipic acid was chosen because it is a commodity chemical used in manufacturing nylon. However, it tends to agglomerate. A number of experiments were performed under different conditions. The saturation temperature chosen for all the experiments was 40°C, and the solubility of adipic acid in water at this temperature is 5.12 g of salt per 100 g of water (Seidell, 1941). The stirrer speed used was 250 rpm and the experiments were performed at various cooling rates ranging from 0.1°C/min to 10°C/min. However, there was significant agglomeration in all cases. A typical agglomerate is shown in Figure 8. Due to the severe agglomeration, this system was abandoned as a test system.

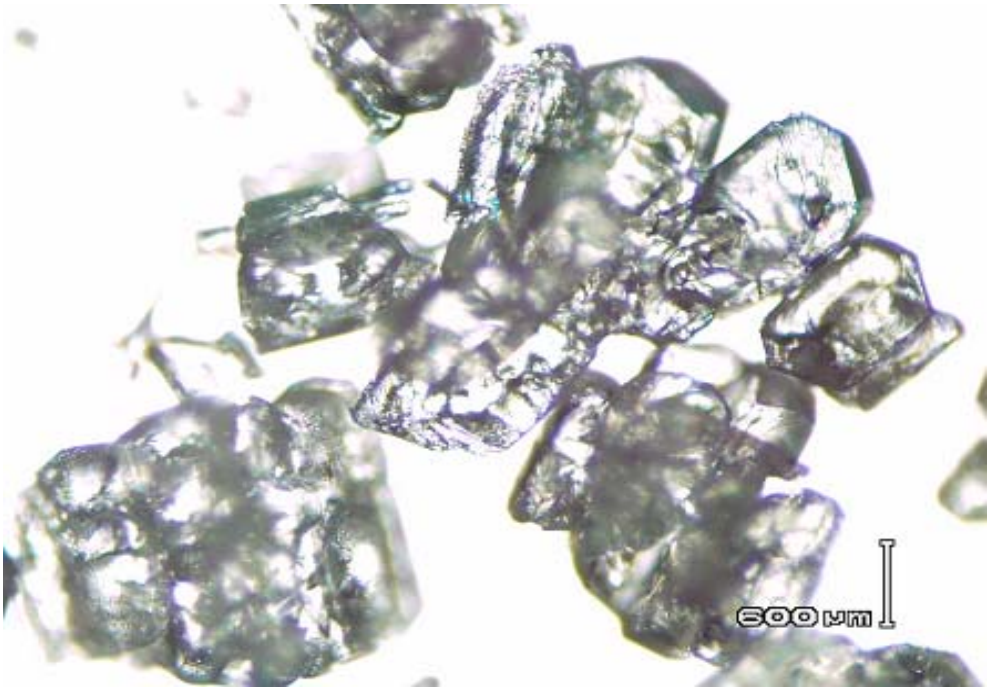

Figure 8: An image of adipic acid crystal taken at 100x magnification

4.2 Ammonium sulfate

Ammonium sulfate was also considered as a compound for investigation. The solubility of ammonium sulfate at 40°C is 162g/100g of water (Seidell, 1928). The saturation temperature of 40°C was used for all the experiments. Several sets of experiments were performed using distilled and deionized water.

Crystallization Experiments for Ammonium Sulfate:

The first set of experiments used distilled water of ASTM-III purity taken from the chemistry lab. Experimental conditions were as shown in Table 3. Seeding for all the experiments were done at 40°C and a stirrer speed of 120 rpm was used for

most of the experiments. By using distilled water, the salt never dissolved even after taking the substance to 10°C above the saturation temperature of 40°C and keeping it at that temperature for about 24 hours. This is shown in Run 7 of Table 3, where the reactor was maintained at 50°C for 840 min and still the contents were not dissolved completely. Since ammonium sulfate was not readily soluble in water, one full day was required to carryout each of these experiments. In each case, the solution was taken above the saturation temperature and kept at that temperature for at least 6 hours. The same result was obtained even after making successive runs using distilled water. A few experiments were repeated keeping the same operating conditions as shown in Table 3 for reproducibility but the results were never consistent due to reasons explained latter.

As far as the crystal shape was concerned, needles or rods were formed under slow cooling rates 0.1°C/min, 0.5°C/min, and 0.2°C/min; and chunky crystals were formed under higher cooling rates of 1°C/min or 1.5°C/min. Sometimes a mixture of both was obtained.

Mullin, et al., (1970) worked on the nucleation and growth of ammonium sulfate crystals from aqueous solution and mentioned the use of deionized water for their experiments. This led us to conclude that ammonium sulfate is very sensitive to even trace amount of ions present in water. Although other researchers (Kitamura, Ikemoto, Kawamura and Nakai, 1992) discussed the effect of ions on shape of crystals formed, no literature was found on the effect of ionic impurities on the solubility of ammonium sulfate. In general if an impurity is present in a saturated binary solution, it may either react chemically with the solute to alter the nature of the

system, or it might make the solution supersaturated with respect to the solute and precipitate it, or it might make the solution unsaturated with respect to the solute. The former phenomenon is termed as ‘salting-out’ while the later one is known as ‘salting-in’ (Mullin, 2001). Since ions had a strong effect on particle shape, they could also have an effect on solubility.

Table 3: Experiments for ammonium sulfate conducted with distilled water

Test Number	Cooling rate (°C /min)	Stirrer speed (rpm)	Saturation temperature (°C)	Temperature at which samples were taken (°C)
1	0.1	100	40	35
2	0.1	150	40	30
3	0.5	150	40	30
4	0.5	100	40	30
5	0.1	120	40	30
6	0.1	120	40	30
7	0.1	120	40	30 (The reactor was maintained at 50°C for 840 min and still the contents were not dissolved completely).
8	0.33	120	40	30
9	0.2	120	40	30 (crystals never appeared)
10	0.2	120	40	30
11	0.2	120	40	30
12	0.16	120	40	30
13	0.5	120	40	30
14	0.1	120	40	30
15	0.1	120	40	30
16	0.1	120	40	30
17	0.1	120	40	34
18	0.5	120	40	30 (crystals never appeared)
19	0.5	120	40	30
20	0.5	100	40	30
21	0.5	120	40	30
22	0.5	100	40	30

The second set of experiments used deionized water of ASTM-I purity taken from the Hand Chemical Laboratory at Mississippi State University. The experiments performed are shown in Table 4. The deionized water provided improved results as far as the solubility was concerned, but there were problems concerning the crystallization once the solution was cooled. Crystals came out of solution significantly above the saturation temperature during cooling. For example, the first experiment mentioned in Table 4 used a saturation temperature of 40°C and a cooling rate of 1°C/min. For the experiments, the contents were heated up to 60°C to dissolve the ammonium sulfate. Once the solution was observed to be clear, it was cooled to start crystallization. The crystals started appearing at 43°C, which is thermodynamically impossible since the solution is still above the saturation temperature of 40°C. There were many such experiments where the crystals were clearly visible before the solution had cooled to the saturation temperature. This indicated that there was some impurity that was altering the solubility.

Table 4: Experiments for ammonium sulfate performed using deionized water

Cooling rate (°C /min)	Stirrer speed (rpm)	Saturation temperature (°C)	Temperature at which samples were taken (°C)
1	120	40	30
0.2	120	40	30
0.2	120	40	34
0.2	110	40	30
1	120	40	30
0.2	120	40	30
0.2	120	40	30
0.2	120	40	35
0.2	120	40	36
0.2	120	40	34
0.2	120	40	30
0.2	120	40	30
0.2	120	40	30
0.2	120	40	35
0.5	120	40	32
0.5	120	40	30
0.5	120	40	34
0.5	120	40	30
0.4	120	40	34

The concern was that impurities from another source were contaminating the system. Cleaning the reactor completely did not improve the results either. Another problem was that the crystals never appeared in some experiments even after taking the solution from 15°C to 20°C below the saturation temperature. Larson and Mullin (1973) observed that metastable zones widen in the presence of impurities for ammonium sulfate. This was specifically found in the presence of chromium ion impurity. But in our case the reactor was cleaned with distilled water and then rinsed with deionised water to avoid adding any impurities.

Since seeding a metastable solution can cause crystallization, the reactor was seeded at 40°C, which was the saturation temperature. But seeding the reactor did not give consistent results either. That is, the results were not reproducible. The shape of the crystals was a rod one time, chunky the next time and sometimes there was a combination of both.

4.3 Urea

Urea is a large commodity chemical that is used in fertilizer production. Unlike ammonium sulfate, urea was not as prone to solubility problems due to impurities and was readily soluble in water. The solubility data was taken from Siedell (1928). But urea had its own problem, which made it a difficult compound to work with. The growth rate was very high for urea and it produced long needles that readily broke. Toyokura and Ohki (1991) investigated the latitudinal and longitudinal growth of single crystal of urea. They found that urea crystals had the tendency to break since they formed needles and so accounted for breakage while modeling the growth rate. The same problem was encountered in the present work. The size of the crystals was longer and broke a lot due to which representative data were not obtained. The cooling rate, sample temperature and the stirrer speed was changed to see how much the variation affected the growth and the shape. Table 5 shows the experiments that were conducted at a saturation temperature of 30.7°C with a stirrer speed of 100 rpm. The seeding temperature was 29°C for these experiments. About 0.04 g of urea was seeded in the reactor for all the experiments at 29°C. This table

also shows the resulting mean area, major axis, minor axis and aspect ratio that were obtained.

Table 5: Data taken for urea at 100 rpm

Cooling rate °C/min	Sample Temperature °C	Area (μm^2)	Aspect ratio	Major axis (μm)	Minor axis (μm)
1.4	28.5	3080.02	8.57941	182.111	24.8431
1.4	28	3174.86	10.381	201.204	22.4922
1.4	27	3249.11	11.6275	223.102	20.48
1.2	28	2769.13	13.0088	190.591	19.8271
1.2	28	3101.16	9.20875	188.171	23.7978
1.2	27	2557.92	13.2881	190.565	18.445
1.2	27	4710.3	7.66492	214.388	30.9554
1.2	26	3675.44	10.6709	200.467	21.8702
1.2	26	5711	9.45679	256.801	29.1972

As seen from the Table 5 there was a strong deviation in the data obtained at 27°C and 26°C at 1.2°C/min repeated tests. At 1.4°C/min though, an increase in major axis was found as the temperature was decreased from 28.5°C to 27°C. The images of the crystals show that breakage had occurred which made it difficult to determine the actual growth of crystals as shown in Figure 10.

Table 6 shows the experiments that were conducted at a saturation temperature of 30.7°C with a stirrer speed of 150 rpm at cooling rates of 1.2°C/min and 1.4°C/min. The experiments were seeded at 29°C. There was not much increase in length from 28°C to 27°C. For 1.2°C/min the length was almost the same as shown in the Table 6, so a definite growth pattern was not seen with the experiments that were performed for urea. This is probably due to the breakage of the long

needles. Also, as shown in Figure 9, there were many crystals that grew much longer and extended out of the microscope's field of vision.

Table 6: Data taken for urea at 150 rpm

Cooling rate °C/min	Sample Temperature °C	Area (μm^2)	Aspect ratio	Major axis (μm)	Minor axis (μm)
1.4	28	4860.52	10.1034	250.969	26.6197
1.4	27	6462.99	8.35605	257.617	32.5911
1.2	28	4971.38	10.1933	239.508	28.8267
1.2	27	5071.87	7.96911	240.887	30.3017

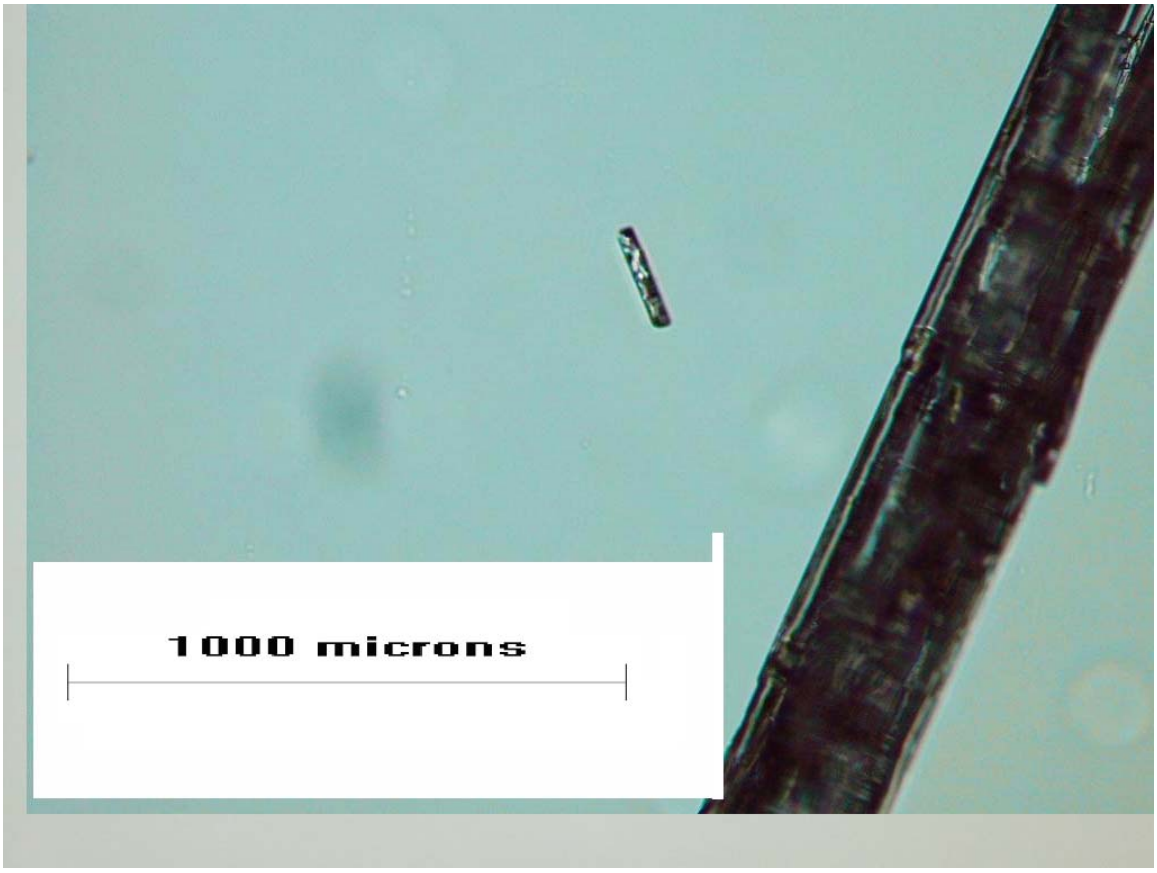

Figure 9: Photograph of urea crystal taken at 100x magnification indicating that the growth is too large and crystal is out of field of vision in microscope

Figure 10: The image of a broken urea crystal caused primarily due to excess growth rate

4.4 Glutamic acid:

Glutamic acid is another compound that is studied in this thesis. As discussed in the literature review section, many researchers have studied the two different polymorphic forms of glutamic acid. Unlike ammonium sulfate, glutamic acid is not that sensitive to impurities. The solubility of L-glutamic acid at 69°C is 3.815 g per 100 g of water (Seidell, 1941). Deionized water is used to prepare the solution. Since the β form of glutamic acid was desired, a higher saturation temperature and a lower cooling rate were used as mentioned in the literature (Mougin, Wilkinson, and Roberts, 2002).

Solubility experiments were run and it was determined that although our data was close to the literature data, it was a little different. Data obtained for the solubility of L-glutamic acid from the literature is shown in Table 7, and the corrected one that was found by conducting test runs by dissolving know amount of salt in a given amount of solvent at a particular temperature is shown in Table 8. A graphical comparison is shown in Figure 11. As seen from the graph there was a marked difference in the data that were seen in the literature from the one measured. Since the saturation temperature was selected in between 50°C and 75°C the solubility data in this range was alone verified. This range of saturation temperatures was chosen because only at high temperatures the β form was produced.

Table 7: Solubility for glutamic acid in water taken from literature

Temperature °C	Solubility (Seidell, 1941) (gms of glutamic acid per 100 gms of water)
50	2.186
55	2.632
60	3.169
65	3.816
70	4.594
75	5.532

Table 8: Data from the measured value of solubility

Temperature (±) 1°C	Solubility (gms of glutamic acid per 100 gms of water)
53	2.186
58	2.626
63	3.166
69	3.816
75	4.594

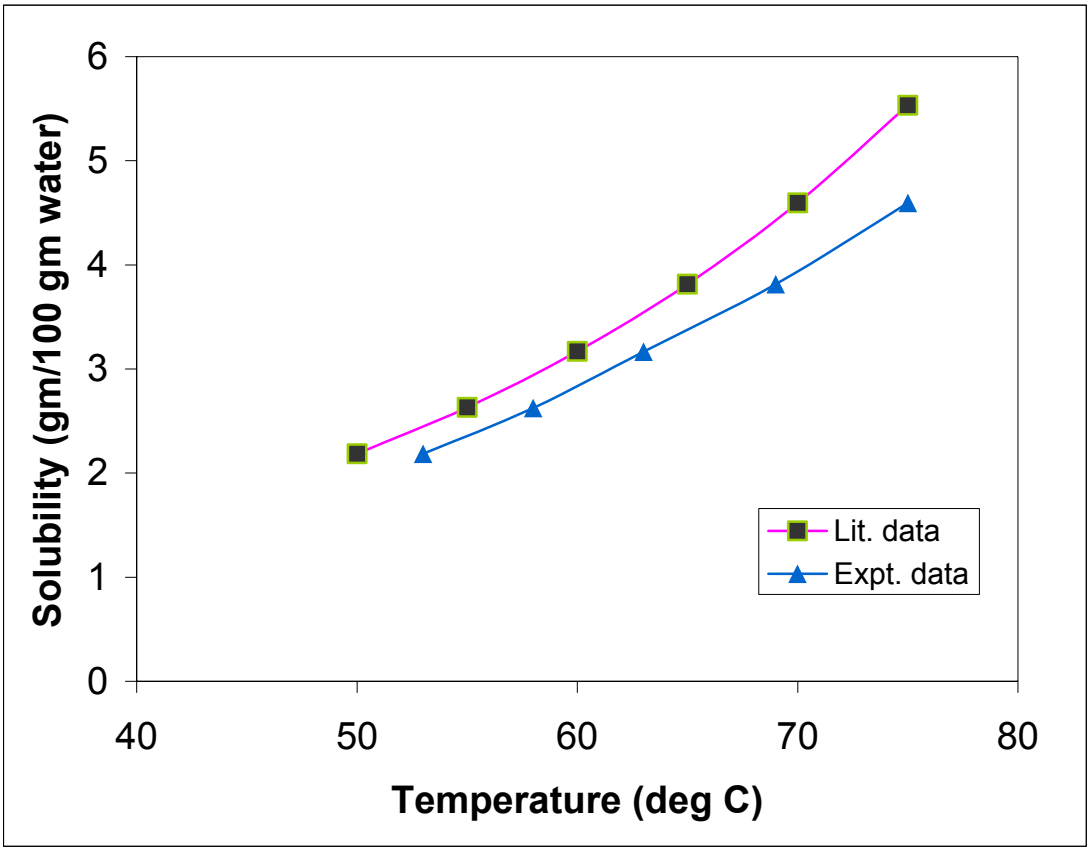

Figure 11: Solubility graph obtained by plotting data from literature and from experiment

For the growth experiments, the crystallization procedure was followed as described in Chapter III. For all of these experiments the saturation temperature was set at 69°C. The solution was taken 10 degrees above the saturation temperature and maintained at that temperature for 30 to 40 min until all the glutamic acid was dissolved and then cooled at the required rate to the temperature desired. Specifically, a cooling rate of 0.5°C/min for all of the experiments that consistently produced the β form. The crystals obtained in all the experiments were needle shaped.

Three sets of tests were done. In the one set of tests the crystallizer was cooled to 63°C, While in the other two sets of tests the crystallizer was cooled to 60°C and to 57°C, respectively. In all of the experiments, crystals were not visible until after the crystallization reached its final temperature. Therefore, it is believed that the crystallization occurred isothermally at the holding temperature.

It was not possible to go below 57°C since the material coming out of solution plugged the crystallizer. This is because increasing the difference between the saturation temperature and the operating temperature increases the driving force. This causes more crystals to nucleate and also causes the existing crystals to grow larger, which essentially causes the plugging in the reactor. Also, a sample could not be taken above 63°C as hardly any sample was observed coming out of solution above that temperature.

The samples were withdrawn after crystallizing at a constant temperature for various holding times ranging from 50min to 240min. Experiments did not continue beyond 240 minutes because the sample coming out of solution caused the crystallizer to plug at the bottom. Experiments were not conducted below 50 minutes because there were not any visible crystals inside the reactor before this time. When samples from residence times less than 50 minutes were filtered, no solid sample was recovered. At each holding time and operating temperature, the experiments were repeated thrice in order to account for repeatability. Approximately 0.0125 g glutamic acid was added for seeding at the saturation temperature. This was added as soon as the solution reached the operating temperature. The purpose of adding the seeds was to obtain more consistent experimental results.

Table 9 shows the data that were obtained at a sample temperature of 63°C and conducted at a cooling rate of 0.5°C/min with a stirrer speed of 120 rpm. The seed crystals were added at 69°C, which is the saturation temperature. The data that were obtained were the area, length of major axis; length of minor axis; and aspect ratio, which is the ratio of major to minor axis.

Glutamic acid showed a consistent increase in the length of major axis with increase in holding time. On the average the aspect ratio was consistently around 10, which indicated the crystals, grew more in length than width.

Table 9: Data for glutamic acid for the sample taken at 63°C

Holding time (min)	Area μm^2	Major Axis μm	Minor Axis μm	Aspect ratio
80	40223.24	648.8798	79.87805	8.905317
80	40339.99	642.4966	84.86349	8.492234
80	29409.91	691.5726	62.40599	11.65798
80	29249.52	674.7487	62.54187	11.63982
80	27825.89	605.0302	63.43458	10.14506
50	23023.76	543.7781	61.25718	9.530274
50	18417.64	496.313	53.99261	9.867308
60	23841.81	558.3976	61.98682	9.662191
60	23790.63	540.4651	62.39064	9.34954
70	29114.77	650.4092	61.85469	11.219
70	28449.37	619.3082	63.33846	10.31351
100	33139.53	697.0728	66.30532	11.10185
100	30733.84	658.7085	65.44908	10.79694
120	43815.81	716.7409	85.69912	9.712942
120	43371.99	740.821	82.30549	10.56276
120	37557.32	761.5259	68.84551	11.89258
180	45825.8	776.4951	83.27558	11.08638
180	39933.85	728.898	78.94642	10.94627
180	41434.13	873.1133	70.84307	14.00121
210	59119.67	928.9241	85.42972	13.54874
210	52330.66	791.3247	95.36911	10.02212
210	40741.88	890.8976	63.26765	15.09118
225	59257.3	852.4814	97.29741	10.65782
225	57904.1	726.424	114.2079	7.586533
225	38937.55	824.6123	63.82938	13.2887
240	60865.76	866.0828	93.33111	11.23848
240	66461.97	792.1932	111.4291	8.414369
240	39958.06	885.6026	65.47786	14.7945

Since for all the experiments the value of major axis never exceeded 1700 μm, the number fraction was obtained by categorizing all the values of major axis between 0 and 1612 μm in 20 intervals using a geometric progression. After calculating the number of samples that belong to particular interval, the number fraction was obtained by dividing the number present in one particular interval by the total number

in the sample. Then the number fraction was plotted against major axis to see the CSD.

As seen in Figure 12a, there is a shift of the peak towards the right as we move from 50 min to 100 min, which indicates growth. But the same pattern was not seen as the time was increased beyond 100min. In Figure 12b for 240 min, a trimodal distribution was obtained. Also the curve for 210 min was not as smooth as the other ones. The physical explanation for the multimodal distributions is that another mechanism other than growth or nucleation has become active. Observation of crystals under the microscope indicated that agglomeration was not occurring. Given the size of the larger crystals, it is quite likely that breakage starts to become significant after 100 minutes. Therefore, only the tests performed at 100 minutes or shorter times are considered in determining the growth and nucleation rates.

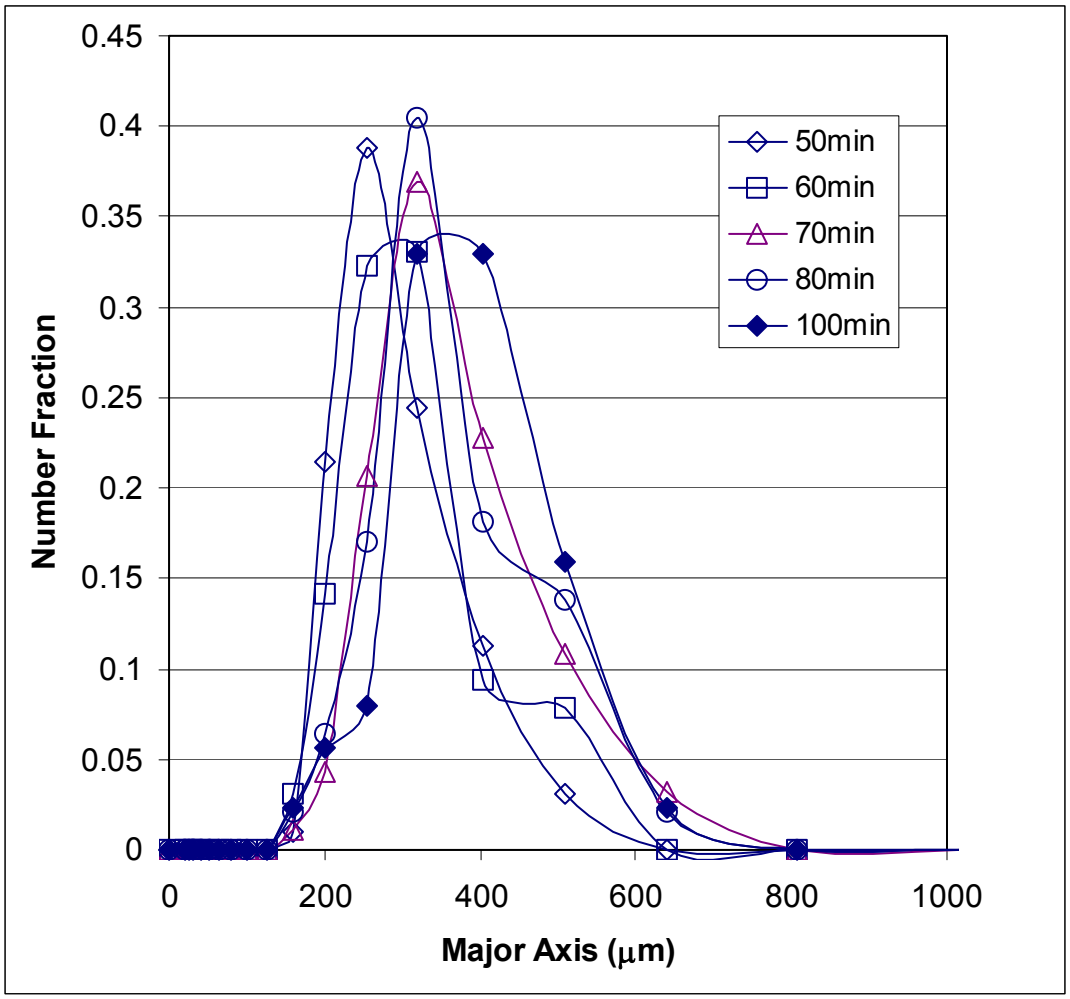

Figure 12a: Plot of number fraction versus major axis for the samples taken at 63°C

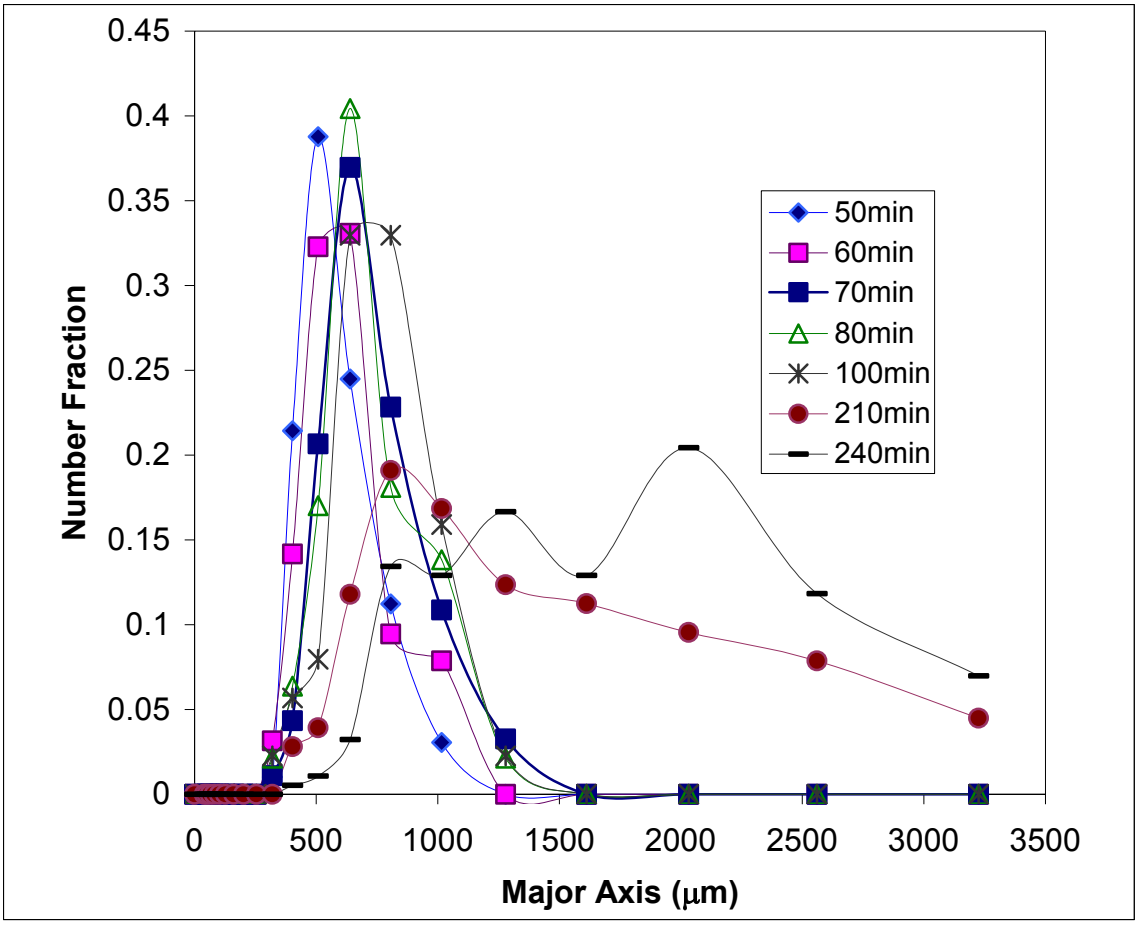

Figure 12b: Plot of number fraction versus major axis for sample taken at 63°C

Table 10 shows the data that were obtained at a sample temperature of 57°C and conducted at a cooling rate of 0.5°C/min with the stirrer speed of 120 rpm. Again the saturation temperature was 69°C and the seeds were also added at the operating temperature.

Table 10: Data for glutamic acid for the sample taken at 57°C

Holding time (min)	Area μm^2	Major Axis μm	Minor Axis μm	Aspect ratio
50	44755.2	831.078	75.8874	11.8357
50	34907.8	760.508	65.9245	12.3103
72	37920.9	564.504	95.3773	7.02758
72	46178.9	881.795	77.1392	12.3869
72	44175.7	877.306	70.7985	13.0001
120	44506.5	552.83	112.552	5.8351
120	44333.9	892.321	71.526	13.0471
120	52036.9	1023.94	71.6297	15.2279
180	46607.4	614.333	103.61	6.92783
180	79012.7	1250.68	87.2577	15.3913
180	58184.5	954.652	87.0078	11.5875
180	53770.6	879.143	81.789	10.6783
210	59093	803.029	103.438	8.68532
210	68602.8	1068.85	89.2554	12.4144
210	64808.6	969.034	90.8662	10.9639
240	89538.6	924.397	119.985	7.95365
240	75154.7	947.621	104.709	9.44554
240	68302.3	1060.22	85.4137	12.8742

In this set of experiments, much higher values of major axis was obtained compared to 63°C as expected. The number fraction plot was plotted in the same manner as explained for 63°C as shown in Figure 13. The aspect ratio was still around 10 for 57°C.

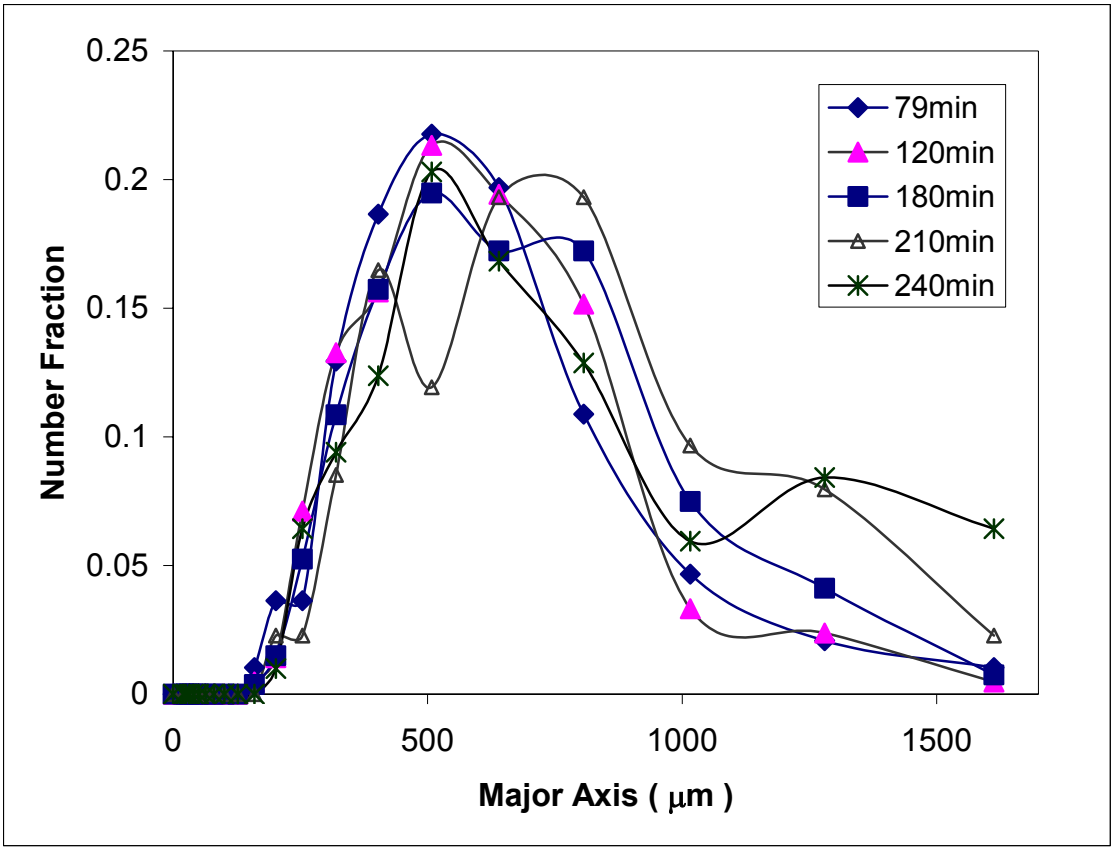

Figure 13: Plot of number fraction versus major axis for sample taken at 57°C

The curves obtained at 57°C were not as unimodal as obtained for 63°C. The curve obtained for 210 minutes was very inconsistent with the distributions at other times. Only the distributions for 79 min and 120 min were unimodal and therefore reasonable for growth and nucleation only. It was hard to see the growth pattern for higher holding time, which was the same case as in 63°C.

For glutamic acid, the density meter was not used for getting the concentration measurements because the data obtained from the density meter was not consistent. So a different method was used to measure the concentration for glutamic acid. Once the experiment was completed and sample was ready for filtration, about 2 ml of sample was taken out using a syringe and transferred to a plastic weighing dish that

had already been weighed. The weight of the sample taken was measured. Then the plastic dish was placed in an oven for about 6 hours to evaporate the water. Once the water was evaporated the weight of the solid alone was measured. From this we can calculate the amount of glutamic acid that was present in the solution at the end of experiment. Since the initial concentration was known, the amount of material that came out of solution could be calculated.

Figure 14 shows the plot of supersaturation versus time obtained for a sample taken at 63°C. The concentration was measured to be 0.4325 g per 100 g of solution at 50min holding time, and 0.0549 g per 100 g of solution at 100 minute holding time. There was a decrease in supersaturation value as the residence time increased from 50 min to 100 min. But the data obtained at 70 min and 90 min varied significantly and did not follow this trend. But the other four points clearly showed the decrease in supersaturation as the holding time was increased. Since the sample was taken down from the reactor conditions to the room temperature there was continuous evaporation taking place during the weighing. Even a loss of 0.025 g of sample increased supersaturation measurement by 0.1 g per 100 g of solution. Therefore the accuracy is ± 0.1 g per 100 g of solution. So, evaporation of the sample affected the concentration data obtained.

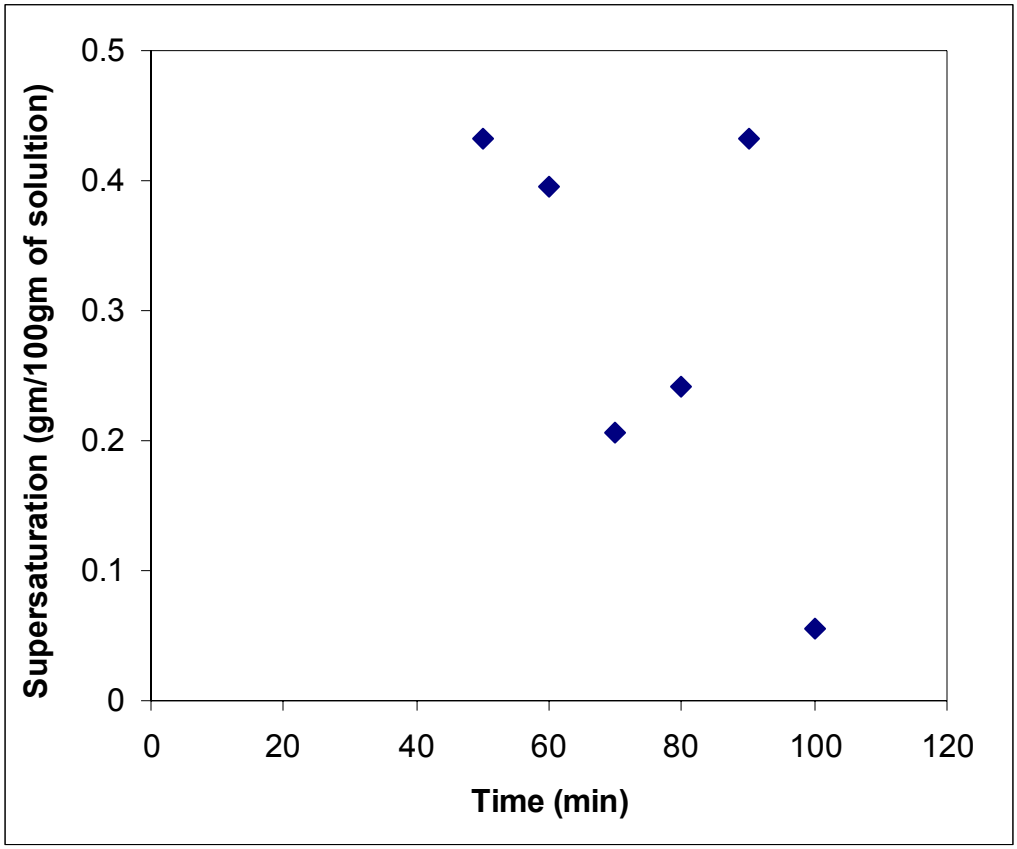

Figure 14: Plot of supersaturation versus time for a sample at 63°C

Figure 15: Image of glutamic acid taken at 100x magnification

It is insufficient to do an experiment once. Experiments must be done several times to determine repeatability. Tabulated data for tests at 57°C are shown in Table 10. Figure 16 shows these graphically. These show the average value of the major axis of the crystals as a function of residence time in the crystallizer. While there is good agreement at 50 minutes, the values diverge at longer times. However, the divergence is smaller for the 2D area of the crystals as shown in Table 12 and Figure

17. This 2D area is the area seen in a 2 dimensional image. Also, less divergence is seen for the minor axis of the crystals as shown in Table 13 and Figure 18.

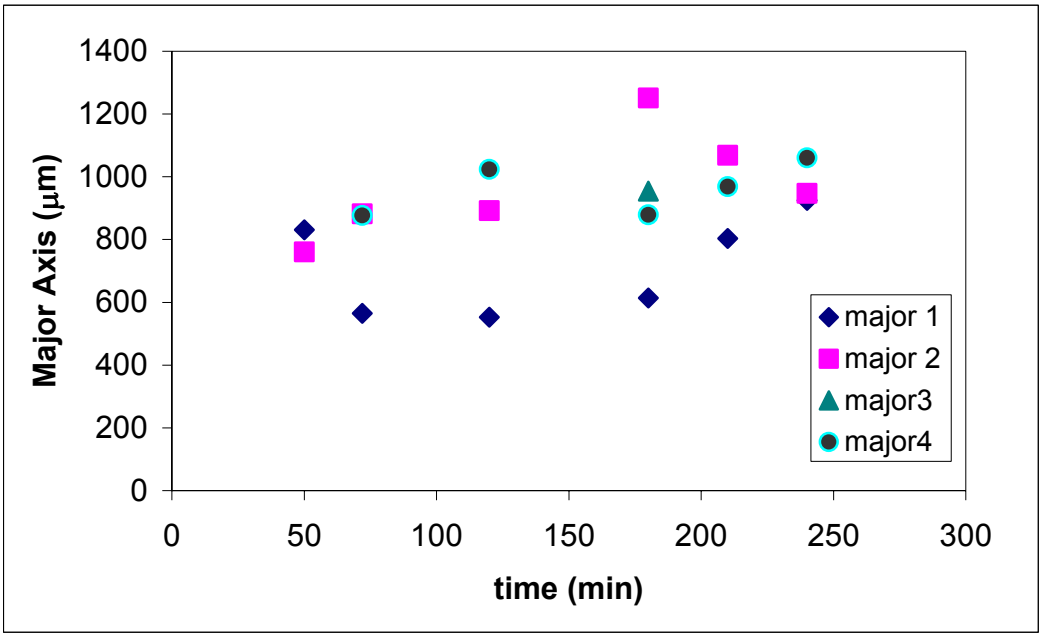

Figure 16: Plot of Major axis versus different holding time for sample taken at 57 °C

Table 11: Major axis data for glutamic acid at 57°C

Time (min)	Major axis 1 (µm)	Major axis 2 (µm)	Major axis 3 (µm)	Major axis 4 (µm)
50	831.0777	760.5076		
72	564.504	881.295		877.306
120	552.8297	892.3212		1023.936
180	614.3333	1250.684	954.6517	879.1427
210	803.0289	1068.846		969.0342
240	924.3968	947.6211		1060.216

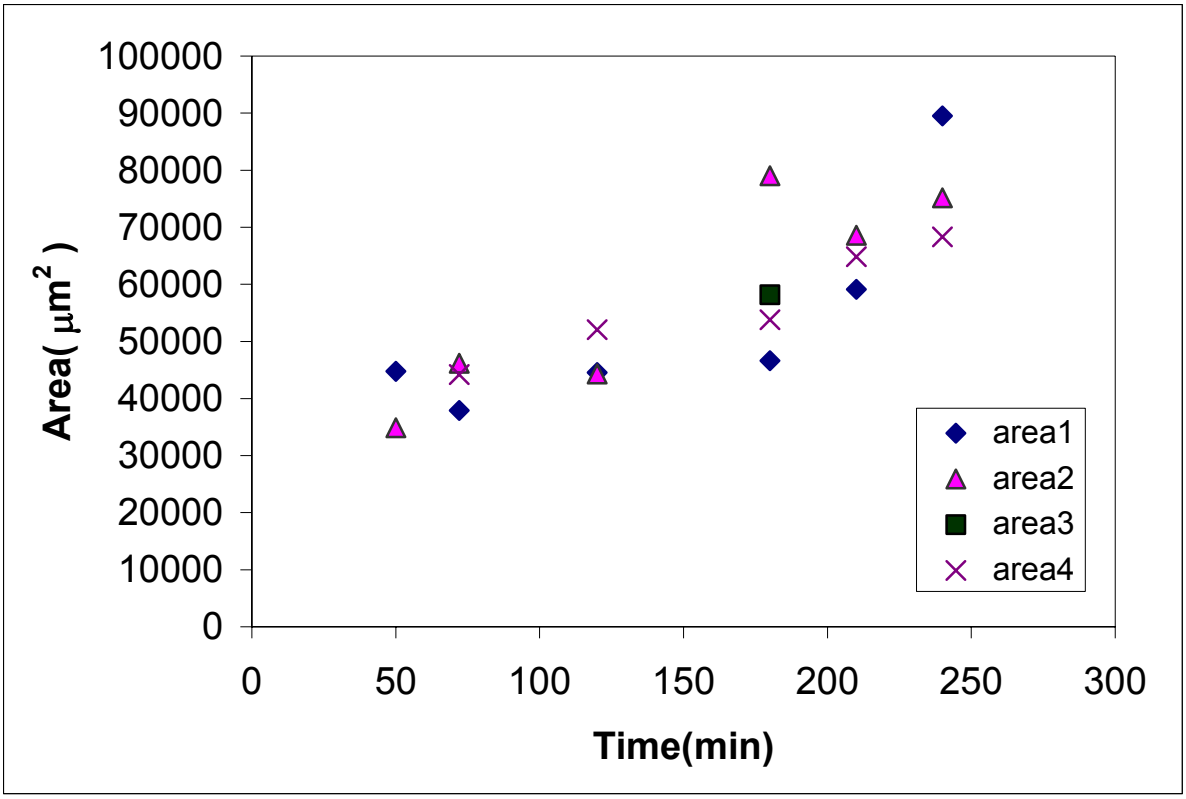

Figure 17: Plot of area versus different holding time for sample taken at 57°C

Table 12: Area data for glutamic acid at 57°C

Time (min)	Area 1 (μm^2)	Area 2 (μm^2)	Area 3 (μm^2)	Area 4 (μm^2)
50	44755.18	34907.78		
72	37920.93	46178.85		44175.71
120	44506.46	44333.94		52036.95
180	46607.45	79012.72	58184.47	53770.6
210	59092.98	68602.85		64808.64
240	89538.63	75154.71		68302.26

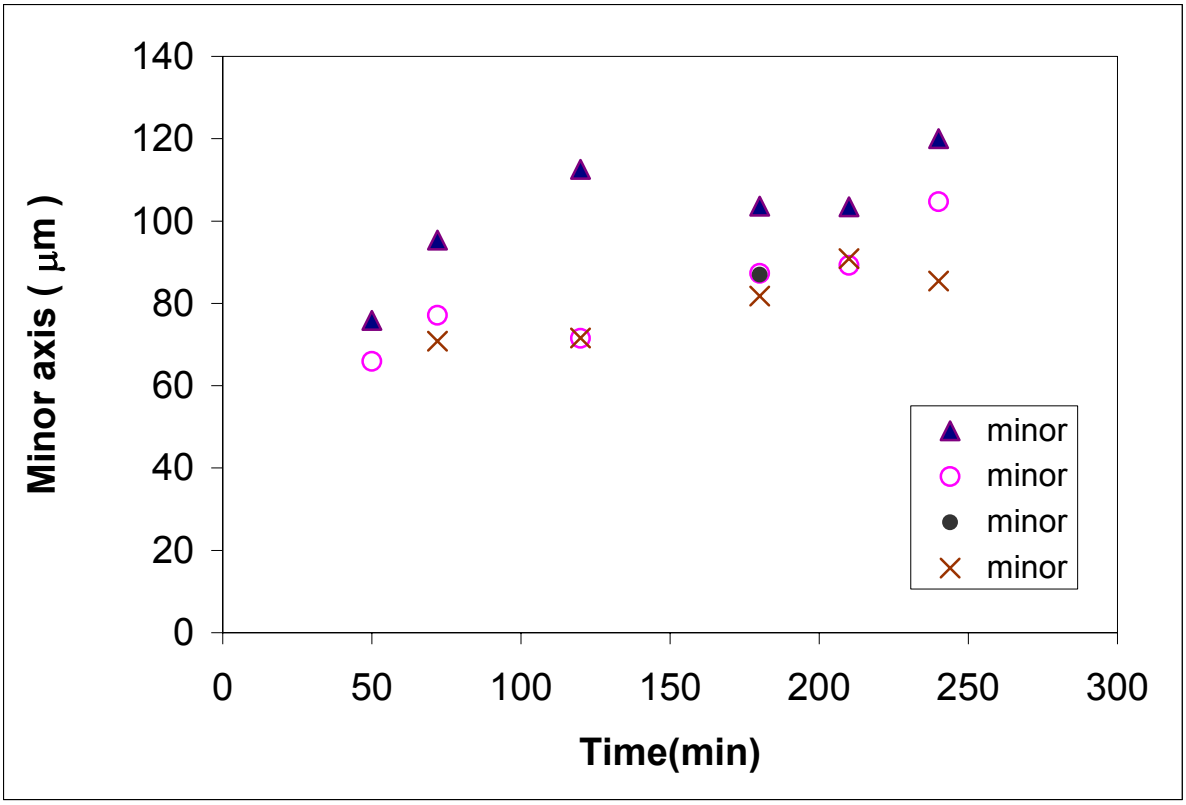

Figure 18: Plot of minor axis versus different holding time for sample taken at 57°C

Table 13: Minor axis data for glutamic acid at 57°C

Time (min)	Minor axis (µm)	Minor axis (µm)	Minor axis (µm)	Minor axis (µm)
50	75.88738	65.92453		
72	95.37726	77.13921		70.79852
120	112.5518	71.52601		71.62971
180	103.6103	87.25769	87.00778	81.78898
210	103.4385	89.25544		90.86617
240	119.9849	104.7087		85.41368

Tabulated data for tests at 63°C are shown in Tables 14, 15 and 16 for the major axis, 2D area, and minor axis, respectively. Results are shown graphically in the corresponding Figures 19, 20 and 21. Comparing Figure 19 at 63°C with Figure

16 at 57°C, it is clear that there is much less scatter in the data for residence times of 120 minutes or less. Specifically, at 120 minutes and 57°C, the ratio of the largest average major axis to the smallest average major axis is approximately 1.85. For the corresponding case at 63°C, this ratio is approximately 1.062. Therefore, the data at 63°C is more reliable for residence times of 120 minutes or less. A similar improvement can be seen for the minor axis where the ratio at 57°C of 1.57 improves to 1.25 at 63°C. However, there is little improvement in the area repeatability where the ratio of the largest average 2D particle area to the smallest average 2D particle area is compared. After 120 minutes of operating time, the area ratio at 57°C is 1.177 and it is 1.167 at 63°C

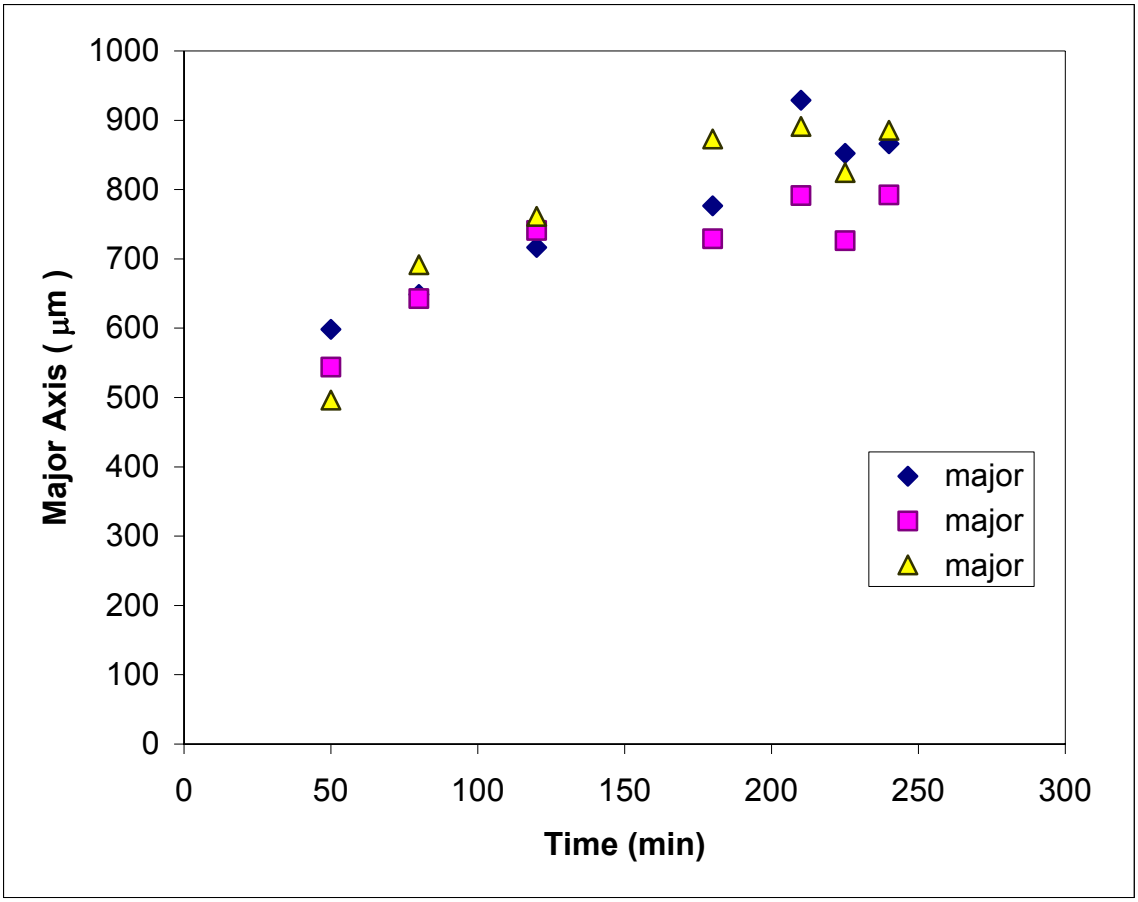

Figure 19: Plot of major axis versus holding time for sample taken at 63°C

Table 14: Major axis data for glutamic acid at 63°C

Time (min)	Major axis (µm)	Major axis (µm)	Major axis (µm)
50	598.3825	543.7781	496.313
80	648.8798	642.4966	691.5726
120	716.7409	740.821	761.5259
180	776.4951	728.898	873.1133
210	928.9241	791.3247	890.8976
225	852.4814	726.424	824.6123
240	866.0828	792.1932	885.6026

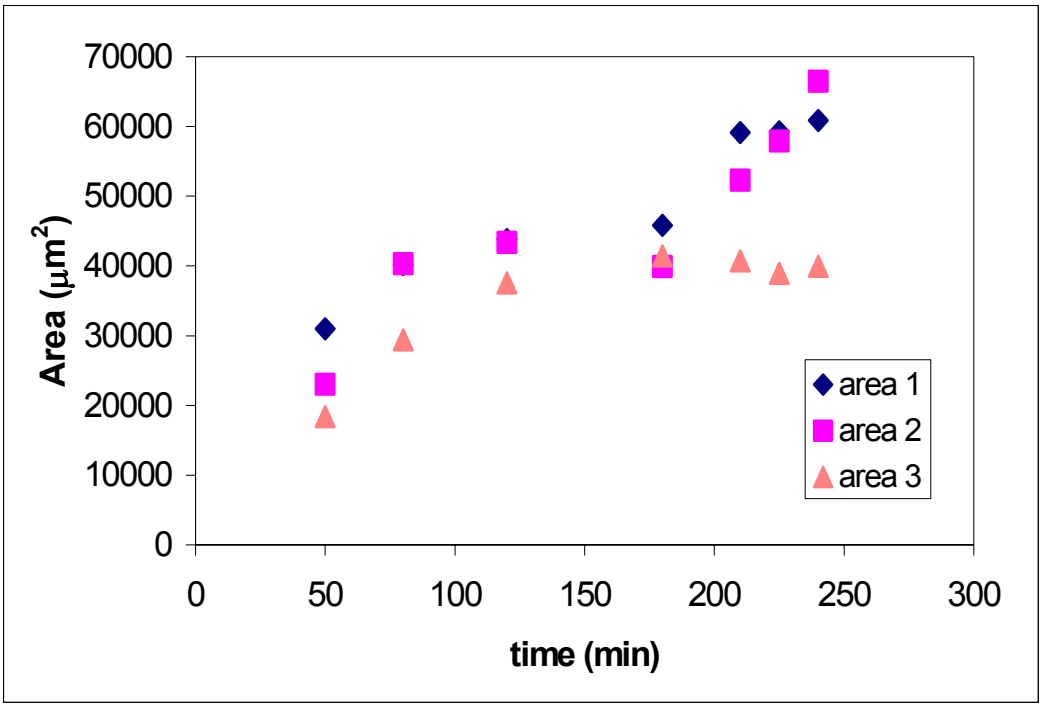

Figure 20: Plot of area versus holding time for sample at 63°C

Table 15: Area data of glutamic acid at 63°C

Time (min)	Area (μm^2)	Area (μm^2)	Area (μm^2)
50	31015.78	23023.76	18417.64
80	40223.24	40339.99	29409.91
120	43815.81	43371.99	37557.32
180	45825.8	39933.85	41434.13
210	59119.67	52330.66	40741.88
225	59257.3	57904.1	38937.55
240	60865.76	66461.97	39958.06

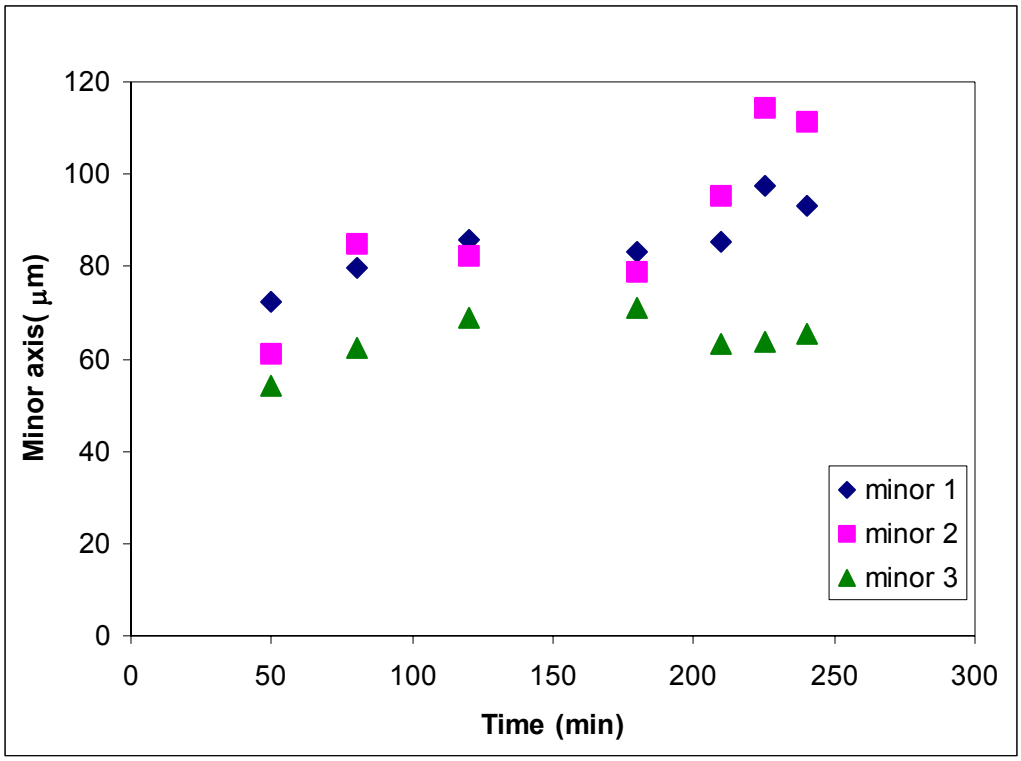

Figure 21: Plot of minor axis versus holding time for 63°C

Table 16: Minor axis data of glutamic acid at 63°C

Time (min)	Minor axis (µm)	Minor axis (µm)	Minor axis (µm)
50	72.41843	61.25718	53.99261
80	79.87805	84.86349	62.40599
120	85.69912	82.30549	68.84551
180	83.27558	78.94642	70.84307
210	85.42972	95.36911	63.26765
225	97.29741	114.2079	63.82938
240	93.33111	111.4291	65.47786

The shape of the crystals did not change much with increase in holding time. Figure 22 shows the plot of aspect ratio versus various holding time. It was found that the aspect ratio was around 10 for all the experiments performed at 63°C at

various holding time. This showed that growth was proportionate in both major axis and minor axis. So, the shape was always needle even when the holding time was increased from 50 minutes to 240 minutes.

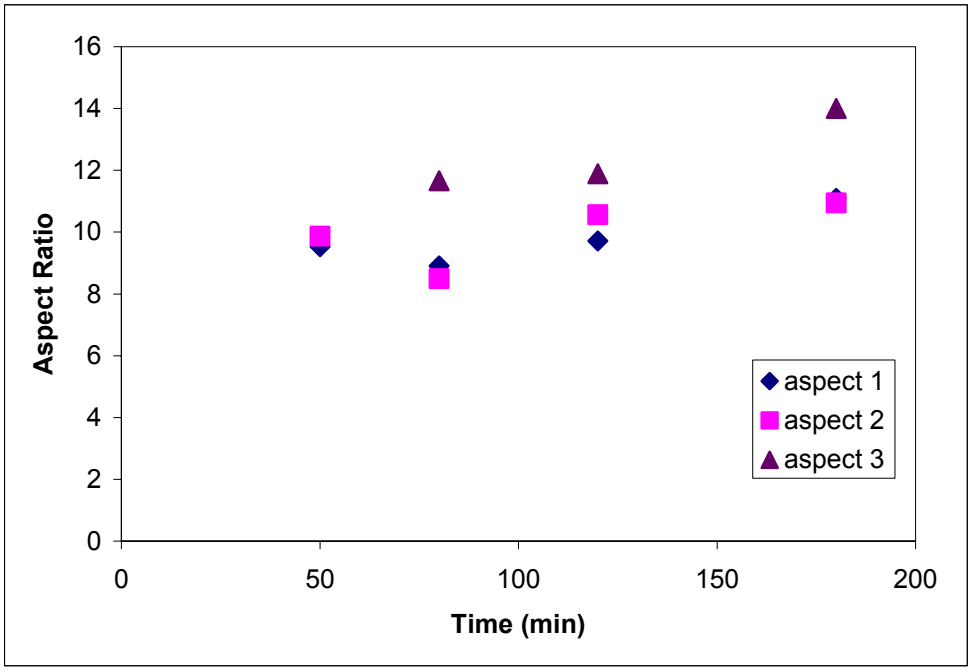

Figure 22: Plot of aspect ratio versus holding time at 63°C

Since the tests at 63°C were the only ones that seemed reliable, they were used for estimating the growth rate. As seen in Figure 23 the shift of the peak for the curves obtained from experimental values is 507 microns corresponding to 50 min to 806 microns corresponding to 100 min. So the growth rate for all the crystals would fall in the range of 3 to 6 microns/min as the holding time is increased from 50 minutes to 100 minutes. The growth rates were also estimated using an already existing model that was incorporated into a numerical simulation by Hill (1996). One difference between this program and other programs is that this program accounted

for the needle shape of the β form of the glutamic acid crystals. Specifically, instead of using the representative diameter of a sphere, the program used the major axis of the particle with a shape factor. Since the data showed that the aspect ratios at 63°C varied around 10, this value was used in the simulation. The program was run using the same parameters as used for the experiment.

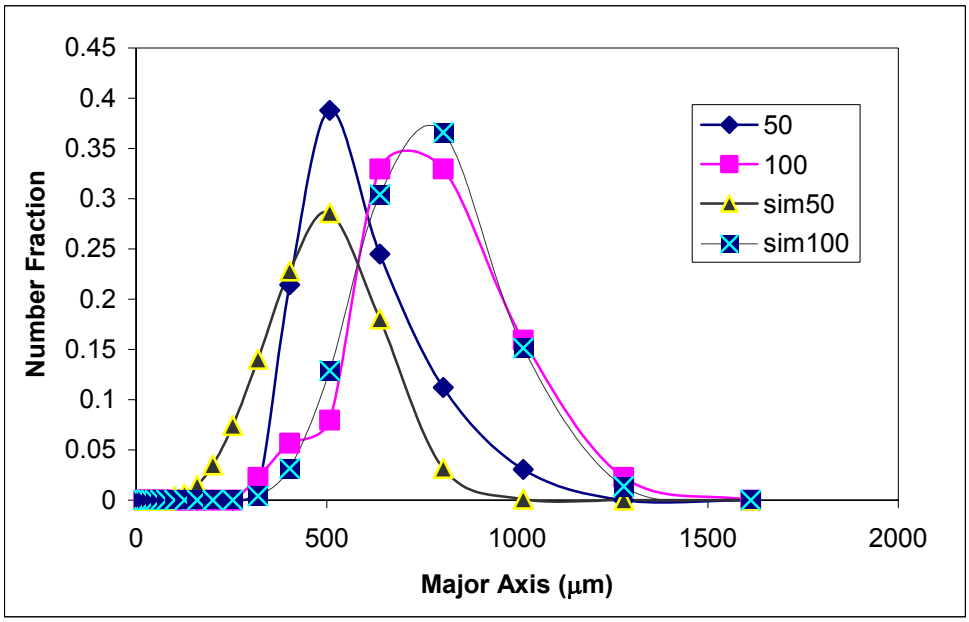

Figure 23: Comparison of number fraction between the experimental values and the values obtained from simulation

The model assumed that breakage and agglomeration were negligible. The growth model used for the simulation was

$$G(L) = g * S^{b} \quad (8)$$

And the rate of nucleation was assumed to be

$$B_0 = c * S^{m} \quad (9)$$

where,

G(L) is the growth rate in microns/min

g is the growth constant

S is the supersaturation in g/liter of solution

b is the growth exponent

B_0 is the rate of nucleation in g/liter of solution

c is the nucleation constant

m is the nucleation exponent

Since it was observed in the experiment that crystals did not appear until the solution had been at 63°C for 13 minutes, the model was set up to have a 13 minute induction period before nucleation began.

A trial and error was used to produce simulation results where the PSD peaks from the simulation are at the same location as those obtained from the experiments. For this condition, the values of growth constant g and growth exponent b are 0.28 μm/min, and 1.4, respectively. The values for the nucleation constant and exponent are 5.6E-18 #/liter/min, and 28, respectively.

In all the cases, the number fraction was plotted at the maximum value of a size interval and the number fraction curve gives the number of particles that fall in this range of maximum value of size intervals. Both the simulation and experimental results are shown in Figure 23. The growth rate of glutamic acid obtained from the simulation varied from 2.53 μm/min at 50 minutes to 0.31 μm/min at 100 minutes. The nucleation rate varies from 0.7356E02 #/liter/min at 50 minutes to 0.3964E-16 #/liter/min at 100 minutes. This is a significant decrease in the nucleation. However, as shown in Figure 23, there aren't any particles smaller than 400 μm after 50

minutes of crystallization. This indicates that nucleation has slowed substantially. Some of the error may be due to the fact that despite the low nucleation rates used in the simulation, the simulation may still be using higher nucleation rates than those actually seen in the experiment.

CHAPTER V

CONCLUSION

Experiments were performed with ammonium sulfate, urea and glutamic acid to investigate crystal growth rate and the effect of processing conditions on crystal shape.

Ammonium sulfate was very sensitive to the ions present in the water. Even using ASTM-1 standard deionized water did not yield consistent results, so it was not possible to measure the growth of ammonium sulfate crystals. It is essential to measure all the ions present in the water used and the effect of these ions on the crystallization of ammonium sulphate in order to measure the growth of ammonium sulphate.

Urea was tried next and urea was not sensitive to impurities. But the growth rate of urea was much higher. The crystals were much longer even for a solution saturated at 30.7°C and the sample taken at 28.5°C, 28°C and 27°C. It was hard to go below that temperature as there was plugging of the reactor. Due to excessive growth either the crystals broke due to agitation in the reactor or it was hard to take pictures for analysis. So urea also failed to produce consistent results.

Finally glutamic acid was tried as a third compound in this thesis. Glutamic acid was also not sensitive to any form of impurity. Instead of changing the cooling

rate and stirrer speed, the holding time was varied. CSD was measured for various holding times to determine the crystal growth rate. As seen in the results chapter, there was a definite increase in the growth of crystals as the residence time was increased from 50 minutes to 100 minutes. However, beyond 100 minutes there was some inconsistency in the data obtained. This could be due to the fact that crystals grew longer with time and started to break, which yielded trimodal distribution for 240 minutes. The same was the case for all the experiments where the sample was drawn at 57°C. The growth rate of glutamic acid was in the range of 3 to 6 microns/min for a change in holding time from 50 min to 100 min at 63°C. The value obtained from the simulation varied from 2.53 μm/min at 50 minutes to 0.31 μm/min at 100 minutes.

The present work on glutamic acid would provide enough preliminary data to further investigate the growth rate of glutamic acid. In the present work with glutamic acid, only the holding time was changed keeping all the other operating parameters constant. In all the cases, rod or needle shaped crystals were obtained; this is the β form of glutamic acid. The experiments were conducted at 0.5°C/min for all the experiments. It would be interesting to study the growth at increased cooling rates at the same saturation temperature to determine whether the β form needles or α form prismatic crystals are formed.

REFERENCES

Abegg, C. F., J. D. Stevens and M. A. Larson, "Crystal size distributions in continuous crystallizers when growth rate is size dependent," *AIChE J*., 14, 1, 118-122 (1968).

Bamforth, A. W., "Crystals and crystalliser systems," *The Chemical Engineer*, August, 287-288, 455- 457 (1974).

Botsaris, G. D., E. G. Denk and J. O. Chua, "Nucleation in an impurity concentration gradient-A new mechanism of secondary nucleation," In Joseph Estrin (Eds.), "Crystallization from Solution: Nucleation Phenomena in Growing Crystal Systems," *AIChE symposium series*, 68, 121, 21-30 (1972).

Buffham, B. A., "The size and compactness of particles of arbitrary shape: application to catalyst effectiveness factors," *Chem. Eng. Sci*., 55, 5803-5811 (2000).

Cise, M. D., and A. D. Randolph, "Secondary nucleation of potassium sulfate in a continuous flow, seeded crystallizer," In J. Estrin (Eds.), "Crystallization from Solution: Nucleation Phenomena in Growing Crystal Systems," *AIChE symposium series*, 68, 121, 42-56 (1972).

Clontz, N. A., and W. L. McCabe, "Contact nucleation of magnesium sulfate heptahydrate," In M. A. Larson (Eds.), "Crystallization from Solution: Factors Influencing Size Distribution," *AIChE symposium series*, 67, 110, 6-17 (1971).

Garside, J., and Mukund B. Shah, "Crystallization kinetics from MSMPR crystallizers," *Ind. Eng. Chem. Proc. Des. Dev.*, 19, 509-514 (1980).

Genck, W. J., and M. A. Larson, "Temperature effects of growth and nucleation rates in mixed suspension crystallization," In J. Estrin (Eds.), "Crystallization from Solution: Nucleation Phenomena in Growing Crystal Systems," *AIChE symposium series*, 68, 121, 57-66 (1972).

Genck, W. J., "Better growth in batch crystallizers," *Chem. Eng. New York*, 107(8), 90-95 (2000).

Hill, P.J., *Simulation of Solids Processes Accounting for Particle Size Distribution*, Ph.D. Thesis, University of Massachusetts, Amherst, MA (1996).

Kitamura, M., T. Ishizu, "Kinetic effect of L-Phenylalanine on growth process of L-glutamic acid polymorph," *J. Cryst. Growth*, 192, 225-235 (1998).

Kitamura, M., "Controlling factor of a polymorphism in crystallization process," *J. Cryst. Growth*, 237-239, 2205-2214 (2002).

Kitamura, M., T. Ishizu, "Growth kinetics and morphological change of polymorphs of L-glutamic acid," *J. Cryst. Growth*, 209, 138-145 (2000).

Kitamura, M., K. Ikemoto, Y. Kawamura, T. Nakai, "Effect of impurity of Cr^{3+} on crystal-growth process of ammonium sulfate," *Int. Chem. Eng.*, 32, 1, 157-163 (1992).

Kotz, J. C., and K. F. Purcell, "Chemistry and Chemical Reactivity," 2nd edition Saunders college, (1991).

Kubota, N., M. Yokota, J. W. Mullin, "The combined influence of supersaturation and impurity concentration on crystal growth," *J. Cryst. growth*, 212, 480-488 (2000).

Larson, M. A., and John W. Mullin, "Crystallization kinetics of ammonium sulphate," *J. Cryst. Growth*, 20, 183-191 (1973).

Lodaya, K. D., L. E. Lahti, and M. L. Jones, "An investigation in to the nucleation kinetics of urea crystallization in water by means of crystal-size distribution analysis," *Ind. Eng. Chem., Proc. Des. Dev.*, 16, 3, 294-297 (1977).

Maginn, S J., "Characterizing crystal habit and habit modification," *Anal. Proc.*, 30, 453-454 (1993).

Mougin, P., Derek Wilkinson and Kevin J. Roberts, "Insitu measurement of particle size during the crystallization of L-glutamic acid under two polymorphic forms: Influence of crystal habit on ultrasonic attenuation measurements," *Cryst. Growth and Des.*, 2, 3, 227-234 (2002).

Mougin, P., Derek Wilkinson and K. J. Roberts, "Insitu ultrasonic attenuation spectroscopic study of the dynamic evolution of particle size during solution-phase crystallization of urea," *Cryst. Growth and Des.*, 3, 1, 67-72 (2003).

McCabe, W. L., J. C. Smith, P. Harriot, *Unit Operations of Chemical Engineering*, McGraw-Hill, Inc., New York, 5th edition (1993).

Mullin, J. W., *Crystallization*, Butterworth-Heinemann, Oxford, 4th edition (2001)

Mullin. J. W., and J. Nyvlt, "Programmed cooling of batch crystallizers," *Chem. Eng Sci*., 26, 369-377 (1971).

Mullin, J. W., M. Chakraborty and K. Mehta, "nucleation and growth of ammonium sulphate crystals from aqueous solution," *J. Appl. Chem*., 20, December 367-371 (1970).

Pons, M. N., H. Vivier, K. Belaroui, B. Bernard-Michel, F. Cordier, D. Oulhana, J. A. Dodds, "Particle morphology: from visualization to measurement," *Powd. Tech.*, 103, 44-57 (1999).

Pons, M. N., and H. Vivier, "Crystal characterization by quantitative image analysis," In R. Ramanarayanan, W. Kern, M. Larson, and S. Sikdar (Eds.), "Particle Design via Crystallization," *AIChE symposium series*, 87(284), 88-95 (1991).

Price, C. J., "Characterizing crystal habit and perfection: A calibration strategy," *Anal. Proc.*, 30, 449-450 (1993).

Perry, R. H., and D. W. Green, "Perry's Chemical Engineers Handbook," McGraw-Hill International editions, New York, 7th edition (1997).

Rajesh, N. P., C. K. Lakshmana Perumal, P. Santhana Raghavan, P. Ramasamy, "Effect of urea on metastable zone width, induction time and nucleation parameters of ammonium dihydrogen orthophosphate," *Cryst. Res. Technol*., 36, 55-63 (2001).

Rouhi, A. M., "The Right stuff-from research and development to the clinic, getting drug crystals right is full of pitfalls," *Chem. Eng. News*, 24 (2), 32-34 (2003).

Sayan, P., J. Ulrich, "Effect of various impurities on the metastable zone width of boric acid," *Cryst. Res. Technol*., 36, 4-5, 411-417 (2001).

Seidell, A., "Solubilities of Inorganic and Organic Compounds," 2nd ed., Van Nostrand, New York, 1928.

Seidell, A., "Solubilities of Organic Compounds," 3rd ed., Van Nostrand, New York, 1941.

Strickland-Constable, R. F., "The breeding of crystal nuclei-A review of the subject," In J. Estrin (Eds.), "Crystallization from Solution: Nucleation Phenomena in Growing Crystal Systems," *AIChE symposium series*, 68, 121, 1-7 (1972).

Toyokura, K., and K. Ohki, "Size distribution of needle crystals of urea obtained from an MSMPR crystallizer," *Int. chem. Eng.*, 31, 3, 493-500 (1991).

Winn, D., and M. F. Doherty, "A new technique for predicting the shape of solution-grown organic crystals," *AIChE J.*, 44, 11, 2501-2514 (1998).